AC SAF ORR VALIDATION REPORT

Validated products:

Name	Acronym
Near-Real-Time Total NO2, GOME-2/Metop-C	NTO/NO2
Offline Total NO2, GOME-2/Metop-C	OTO/NO2
Near-Real-Time Tropospheric NO2, GOME-2/Metop-C	NTO/NO2Tropo
Offline Tropospheric NO2, GOME-2/Metop-C	OTO/NO2Tropo

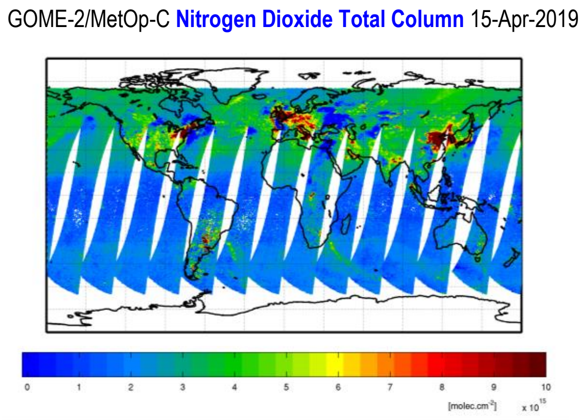

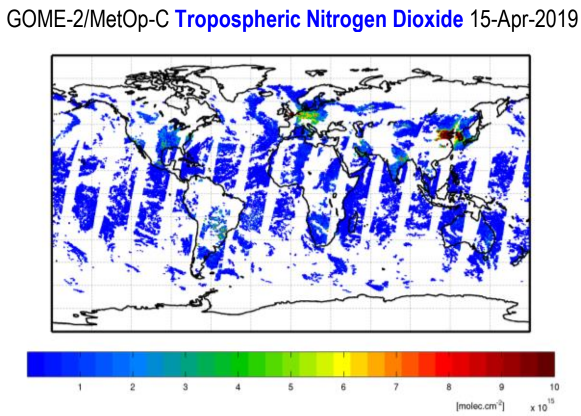

Authors:

Name	Institute
Gaia Pinardi	Royal Belgian Institute for Space Aeronomy
Huan Yu	Royal Belgian Institute for Space Aeronomy
Jean-Christopher Lambert	Royal Belgian Institute for Space Aeronomy
José Granville	Royal Belgian Institute for Space Aeronomy
Jeroen van Gent	Royal Belgian Institute for Space Aeronomy
Michel Van Roozendael	Royal Belgian Institute for Space Aeronomy
Pieter Valks	German Aerospace Center

Reporting period: February 2019 – July 2019

Input data versions: GOME-2 Level 1B version 6.3

Data processor versions: GDP version 4.9, UPAS version 1.4.0

authors G. Pinardi, H. Yu, J.-C. Lambert, J. Granville, Jeroen van Gent, M. van Roozendael, and P. Valks

contributeurs S. Colwell, V. Dorokhov, A. Elokhov, C. Fayt, M. Gil, F. Goutail, A. Gruzdev, G. Hansen, F. Hendrick, C. Hermans, G. Held, N. Jepsen, R. Kivi, K. Kreher, D. Loyola, Navarro, A. Pazmiño, J.-P. Pommereau, T. Portafaix, O. Puentedura, E. Quel, R. Querel, A. Richter, V. Semenov, K. Strong, G. Vaughan, F. Wittrock, and M. Yela

edited by G. Pinardi, BIRA-IASB, Brussels, Belgium

document type AC SAF Validation Report
issue 1
reference SAF/AC/IASB/VR/NO2/ValidationReport_NO2_ORR_MetopC
revision 0
date of issue 25 November 2019
products MCG-O-NO2, MCG-N-NO2, MCG-O-NO2TR, MCG-N-NO2TR
product version level-0-to-1 v6.3, level-1-to-2 GDP v4.9

distribution

Function	***Organisation***
AC SAF	EUMETSAT, BIRA-IASB, DLR, DMI, DWD, FMI, HNMS/AUTH, KNMI, LATMOS, RMI
GOME Team	DLR, ESA/ESRIN, BIRA-IASB, RTS, various
UPAS Team	DLR-IMF, DLR-DFD
NDACC UVVIS Working Group	BAS-NERC, BIRA-IASB, CAO, CNRS/IPSL/LATMOS, DMI, FMI-ARC, IFE/IUP, INTA, IPMet/UNESP, KSNU, NIWA, U. Manchester, U. Réunion/LACy, U. Wales
Ground-based data providers	NIDFORVAL partners

external contributors

NDACC teams contributing ground-based correlative measurements

Acronym	***Organisation***	***Country***
BAS-NERC	British Antarctic Survey – National Environment Research Council	United Kingdom
BIRA-IASB	Royal Belgian Institute for Space Aeronomy	Belgium
CAO	Central Aerological Observatory	Russia
CEILAP	UNIDEF-MINDEF / Centro de Investigaciones en Láseres y Aplicaciones	Argentina
CNRS/LATMOS	CNRS / Laboratoire Atmosphère, Milieux, Observations Spatiales	France
DMI	Danish Meteorological Institute	Denmark
FMI-ARC	Finnish Meteorological Institute – Arctic Research Centre	Finland
IFE/IUP	Institut für Umweltphysik/Fernerkundung, University of Bremen	Germany
INTA	Instituto Nacional de Técnica Aeroespacial	Spain
IPMet/UNESP	Instituto de Pesquisas Meteorológicas, Universidade Estadual Paulista	Brazil
KSNU	Geophysical Laboratory, Kyrgyz State National University	Kyrgyzstan
NIWA	National Institute of Water and Atmospheric Research	New Zealand
U. Manchester	University of Manchester and University of Wales	United Kingdom
U. Réunion/LACY	Université de la Réunion	France
U. Toronto	University of Toronto	Canada

NIDFORVAL teams contributing ground-based correlative measurements

Acronym	***Organisation***	***Country***
BIRA-IASB	Royal Belgian Institute for Space Aeronomy	Belgium
IFE/IUP	Institut für Umweltphysik/Fernerkundung, University of Bremen	Germany
KNMI	Royal Netherlands Meteorological Institute, De Bilt	The Netherlands
MPIC	Max Planck Institute for Chemistry, Mainz	Germany
AUTH	Aristotle University of Thessaloniki, Thessaloniki	Greece
UNAM	Centro de Ciencias de la Atmósfera, Universidad Nacional Autónoma de México	Mexico
UChiba	Center for Environmental Remote Sensing, Chiba University	Japan
LuftBlick	LuftBlick , Kreith	Austria

document change record

Issue	***Rev.***	***Date***	***Section***	***Description of Change***
1	0	24/09/2019	all	Creation of this document
1	1	28/02/2020		Adding AC SAF product ID numbers table

AC SAF product ID numbers

AC SAF internal identifier	***Description***
NRT Total NO2	O3M-338
Offline Total NO2	O3M-339
NRT Tropospheric NO2	O3M-341
Offline Tropospheric NO2	O3M-342

Validation report of GOME-2 GDP 4.9 NO_2 column data for MetOp-C Operational Readiness Review

CONTENTS

ACRONYMS AND ABBREVIATIONS

AC SAF	Atmospheric Composition Monitoring Satellite Application Facility
AMF	Air Mass Factor, or optical enhancement factor
BIRA-IASB	Belgian Institute for Space Aeronomy
CNRS/LATMOS	Laboratoire Atmosphère, Milieux, Observations Spatiales du CNRS
DLR	German Aerospace Centre
DOAS	Differential Optical Absorption Spectroscopy
Envisat	Environmental Satellite
ESA	European Space Agency
EUMETSAT	European Organisation for the Exploitation of Meteorological Satellites
FMI-ARC	Finnish Meteorological Institute – Arctic Research Centre
FRM4DOAS	Fiducial Reference Measurements for Ground-Based DOAS Air-Quality Observations
GDOAS/SDOAS	GOME/SCIAMACHY WinDOAS prototype processor
GDP	GOME Data Processor
GEOMS	Generic Earth Observation Metadata Standard
GOME	Global Ozone Monitoring Experiment
IASB	Institut d'Aéronomie Spatiale de Belgique
IFE/IUP	Institut für Fernerkundung/Institut für Umweltphysik
IMF	Remote Sensing Technology Institute
LOS	Line Of Sight
MAXDOAS	Multi Axis Differential Optical Absorption Spectroscopy
MPC	S5p Mission Performance Centre
Multi-TASTE	Multi-platform Validation System for Technical Assistance To satellite Evaluations
NDACC	Network for the Detection of Atmospheric Composition Change
NDSC	Network for the Detection of Stratospheric Change
NIDFORVAL	S5P NItrogen Dioxide and FORmaldehyde Validation using NDACC and complementary FTIR and UV-Vis DOAS ground-based remote sensing data
NO_2	nitrogen dioxide
O_3	ozone
OCRA	Optical Cloud Recognition Algorithm
OMI	Ozone Monitoring Instrument
PGN	Pandonia Global Network
QA4ECV	Quality Assurance for Essential Climate Variables
ROCINN	Retrieval of Cloud Information using Neural Networks
RRS	Rotational Raman Scattering
RTS	RT Solutions Inc.
S5P	Sentinel-5 Precursor
SAOZ	Système d'Analyse par Observation Zénithale
SCD	Slant Column Density
SCIAMACHY	Scanning Imaging Absorption spectroMeter for Atmospheric CHartography
SNR	Signal to Noise Ratio
SZA	Solar Zenith Angle
TEMIS	Tropospheric Emission Monitoring Internet Service
TROPOMI	TROPOspheric Monitoring Instrument
UPAS	Universal Processor for UV/VIS Atmospheric Spectrometers
UVVIS	ground-based DOAS ultraviolet-visible spectrometer
VCD	Vertical Column Densit

INTRODUCTION TO EUMETSAT SATELLITE APPLICATION FACILITY ON ATMOSPHERIC COMPOSITION MONITORING (AC SAF)

Background

The monitoring of atmospheric chemistry is essential due to several human caused changes in the atmosphere, like global warming, loss of stratospheric ozone, increasing UV radiation, and pollution. Furthermore, the monitoring is used to react to the threats caused by the natural hazards as well as follow the effects of the international protocols.

Therefore, monitoring the chemical composition and radiation of the atmosphere is a very important duty for EUMETSAT and the target is to provide information for policy makers, scientists and general public.

Objectives

The main objectives of the AC SAF is to process, archive, validate and disseminate atmospheric composition products (O_3, NO_2, SO_2, BrO, HCHO, H_2O, OClO, CO, NH3), aerosol products and surface ultraviolet radiation products utilising the satellites of EUMETSAT. The majority of the AC SAF products are based on data from the GOME-2 and IASI instruments onboard Metop satellites.

Another important task besides the near real-time (NRT) and offline data dissemination is the provision of long-term, high-quality atmospheric composition products resulting from reprocessing activities.

Product categories, timeliness and dissemination

NRT products are available in less than three hours after measurement. These products are disseminated via EUMETCast, WMO GTS or internet.

- Near real-time trace gas columns (total and tropospheric O_3 and NO_2, total SO_2, total HCHO, CO) and high-resolution ozone profiles
- Near real-time absorbing aerosol indexes from main science channels and polarization measurement detectors
- Near real-time UV indexes, clear-sky and cloud-corrected

Offline products are available within two weeks after measurement and disseminated via dedicated web services at EUMETSAT and AC SAF.

- Offline trace gas columns (total and tropospheric O_3 and NO_2, total SO_2, total BrO, total HCHO, total H_2O) and high-resolution ozone profiles
- Offline absorbing aerosol indexes from main science channels and polarization measurement detectors
- Offline surface UV, daily doses and daily maximum values with several weighting functions

Data records are available after reprocessing activities from the EUMETSAT Data Centre and/or the AC SAF archives.

- Data records generated in reprocessing
- Lambertian-equivalent reflectivity
- Total OClO

Users can access the AC SAF offline products and data records (free of charge) by registering at the AC SAF web site.

More information about the AC SAF project, products and services: https://acsaf.org/

AC SAF Helpdesk: helpdesk@acsaf.org

Twitter: https://twitter.com/Atmospheric_SAF

DATA DISCLAIMER FOR THE METOP-C GOME-2 TOTAL NO_2 (NTO/OTO) AND TROPOSPHERIC NO_2 (OTR) DATA PRODUCTS

In the framework of EUMETSAT's Atmospheric Composition Monitoring Satellite Application Facility (AC SAF), nitrogen dioxide (NO_2) total and tropospheric column data products, as well as associated cloud parameters, are generated at DLR from MetOp-C GOME-2 measurements using the UPAS environment version 1.4.0, the level-0-to-1 v6.3 processor and the level-1-to-2 GDP v4.9 DOAS retrieval processor (see TN-DLR-ATBD and TN-DLR-PUM). BIRA-IASB, DLR and RMI ensure detailed quality assessment of algorithm upgrades and continuous monitoring of GOME-2 NO_2 data quality with a recurring geophysical validation using correlative measurements from the NDACC ground-based network and from other satellites, modelling support, and independent retrievals.

This report present the initial verification results of MetOp-C GOME-2 NO_2 total and tropospheric data (MCG-N-NO2, MCG-O-NO2, MCG-N-NO2TR, MCG-O-NO2TR) from February to July 2019, by comparisons to MetOp-B results and to available ground-based correlative data. These include:
(1) the verification of the consistency of GDP4.9 GOME-2C NO_2 column retrievals against operational GOME-2B data sets,
(2) the evaluation of the stratospheric contribution to the NO_2 total column against ground-based observations provided by near-real-time DOAS UV-Visible spectrometers of the NDACC network, and
(3) comparisons of tropospheric and total NO_2 column data against ground-based MAXDOAS and Pandora direct-sun measurements coming from the S5PVT NIDFORVAL (S5P NItrogen Dioxide and FORmaldehyde Validation using NDACC and complementary FTIR and UV-Vis DOAS ground-based remote sensing data) project.

The main results are summarized hereafter:

- The GOME-2 C NO_2 slant columns generation from DOAS analysis had to be adapted in version GDP 4.9 to reduce the impact of resolution changes and L1 calibration issues. A fitting window covering 430.2–465nm has been applied to GOME-2C. This leads to geographically coherent slant columns, similar to GOME-2B results, but slightly larger above land and high latitude regions. The slant column scatter is about 10% larger in GOME-2B.
- GOME-2C seems to be less affected by the Southern Atlantic Anomaly (SAA) than previous instruments (better instrument shielding?).
- The systematic bias on the slant columns is transferred to the stratospheric vertical columns. The GOME-2C stratospheric columns are globally larger than GOME-2B, with a latitudinal structure with minimum differences around the equator and an increase at higher latitude (0.5~1e15 molec/cm²).
- Validity of the tropospheric AMF calculation pixels selection has been found to lead to positive bias in the GOME-2B tropospheric columns between 30°S-0°S, leading to biases with GOME-2C. Based on the monthly averaged maps (gridded at 0.5°×0.5°) from February to July 2019, the difference in tropospheric vertical column density between GOME-2B and GOME-2C is ~32% (between 70°S and 70°N, and excluding the SAA regions) for pixels with VCD values exceeding 0.5×10^{15} molecules/cm^2. If only pixels with VCD larger than 2.5×10^{15} molecules/cm^2 are considered, the average difference between GOME-2B and GOME-2C is within 17%. It meets the optimal accuracy of requirement for tropospheric NO_2 (20%).
- The stratospheric NO_2 differences (negative bias over land and high latitudes mainly due to slant column changes) and tropospheric NO_2 differences (positive bias between 30°S and 0° in the average

map related to difference in the data selection criteria) are combined and transferred to the total NO_2 columns. Based on the monthly February to July 2019 averaged data (gridded at 0.5°×0.5°), the difference in total NO_2 vertical column density between GOME-2B and GOME-2C is 2.5×10^{14} molecules/cm^2 (between 70°S and 70°N), which reach the optimal accuracy ($1\text{-}3\times10^{14}$) of the requirement.

- The GOME-2C temporal evolution of the different component of the retrieval is in good agreement with the GOME-2B in average over a few sites with different pollution conditions. Slightly larger differences appear for GOME-2A, probably due to degradation issues and smaller pixels.

- With respect to 14 NDACC ZLS-DOAS UV-visible spectrometers, the MetOp-C GOME-2 GDP 4.9 NO_2 column data, offers the same level of consistency as GOME-2A and GOME-2B GDP 4.8 do. In term of median bias, GOME-2C reports NO_2 column values in most of the cases within $1\text{-}3\cdot10^{14}$ molec.cm-2 from the ground-based values, which is close to the combined uncertainty of ground-based NDACC measurements and of the comparison method. Under many conditions, day-to-day fluctuations of the stratospheric NO_2 column seem to be smoothed by GOME-2C, in comparison to the fluctuations reported by ground-based instruments. Variations of the stratospheric NO_2 column at seasonal scale are captured consistently by all measurement systems. Further investigation based on reprocessed ground-based data with state-of-the-art algorithms needs to be done to confirm current provisional conclusions on GOME-2C data quality and to elucidate apparent dependences on SZA in more difficult conditions.

- Preliminary validation results for GOME-2C and GOME-2B tropospheric and total NO_2 columns are generally very similar, even if the regression parameters can be slightly different. GOME-2 data are able to measure total and tropospheric NO_2 columns and its temporal evolution, especially in sub-urban and remote conditions, while larger under-estimation is found with respect to ground-based MAXDOAS and DirectSun measurements performed in urban environment. This is partially inherent to the large GOME-2 pixel size (40 x 80 km^2), not representative of the local urban NO_2 pattern sampled by the ground-based instruments, as already showed in past validation exercises (NO2 ACSAF VR 2017; Pinardi et al., in preparation). From the MAXDOAS monthly mean values scatter plot, a global correlation coefficient of 0.83 is obtained for GOME-2C, with a slope of about 0.49, strongly influenced by the large ground-based columns in Mexico. Better results are obtained when only focusing in remote and suburban locations, with correlation of 0.92 and slope of 0.75. Compared to Pandora direct-sun measurements, GOME-2C and GOME-2B results are quite coherent, with correlation coefficients of 0.89 and 0.75 and regression slopes smaller than 0.5.

A. INTRODUCTION

A.1. Scope of this document

The present document reports on the verification and preliminary geophysical validation of MetOp-C GOME-2 NO_2 total column data produced over the February-July 2019 time period, namely total (NTO/NO2, OTO/NO2) and tropospheric (NTO/NO2tropo, OTO/NO2tropo) column data. The NO_2 column data are retrieved from GOME-2 spectra by the GOME Data Processor (GDP) version 4.9 operated at DLR in the framework of the EUMETSAT AC SAF. Based on an end-to-end validation approach, this report addresses the quality of individual components of the data processing chain, starting with DOAS spectral fitting results. The report continues with comparisons of GOME-2 final data products with correlative observations acquired by independent ground-based spectrometers and by GOME-2 onboard MetOp-B. The goal is to investigate the consistency of the GOME-2C NO_2 columns and if the product fulfil the user requirements in term of accuracy (for tropospheric NO_2: threshold 50%, target 30% and optimal 20%; for total NO_2: threshold of 1e15 molec/cm² (20% annual mean), target of 3-5e14 molec/cm² (8-15% annual mean) and optimal of 1-3e14 molec/cm² (4-8% annual mean)), as stated in the ACSAF Service Specification Document (https://acsaf.org/docs/AC_SAF_Service_Specification.pdf).

A.2. Preliminary remarks

To report on the status of the verification of the MetOp-C GOME-2 NO_2 columns, in addition to comparisons against GOME-2 on MetOp-B, the consistency of the different NO_2 products is explored by performing comparisons with available correlative data sets. As discussed in detail in Section B2, it should be noted that this part rely on the early delivery of provisional data by network affiliates (e.g. NDACC/UVVIS) or partners within other validation projects (e.g. NIDFORVAL). Results relying on early-delivery data must always be considered as preliminary and more firm conclusions on validation should be updated in the future, to be assembled when more Metop-C measurements will be available (ideally covering at least one year of data).

A.3. Plan of this document

After presentation of the AC SAF introduction and the GOME-2C Data Disclaimer for NO_2 column products, this document is divided into the following sections:

- **A.** This introduction,
- **B.** Validation protocol presenting the method and the reference data used,
- **C.** The verification of the individual components of the MetopC processing chain, with comparisons to MetopB,
- **D.** The evaluation of the NO_2 columns, by comparison with correlative ground-based measurements
- **E.** Conclusions
- **F.** References

B. VALIDATION PROTOCOL

B.1. GDP 4.9 data and validation method

Retrieval principles of GOME-2C NO_2 data are described in the Algorithm Theoretical Basis Document (ATBD, 2019) and the Product User Manual (PUM, 2019) available via the AC SAF web site (https://acsaf.org). Validation method has been set up for the validation of GOME-2A and GOME-2B, and this document is based on the last NO_2 validation report (NO_2 ACSAF VR 2017), but with a more specific focus on establishing the consistency between the GOME-2C and GOME-2B NO_2 product over the 6 month dataset available. The latest GOME Data Processor (GDP), applied to Metop-C, is called version 4.9 due to changes in the SO_2 product; changes are implemented for the adaptation of the NO_2 operational product to Metop-C as well. This product should not be confused with proposed improvements by Liu et al. 2019a and 2019b, for future implementation within the AC SAF.

As before, NO_2 column data are retrieved from the GOME-2 Earthshine backscattered radiance and solar irradiance spectra by several modules calculating intermediate parameters: the apparent slant column density along the optical path (SCD), the fractional cover (CF) and top pressure (CTP) of clouds interfering with the measurement scene, their optical thickness (COT) and albedo (CTA), the geometrical enhancement factor (AMF) needed to convert slant into vertical columns (VCD), and the stratospheric NO_2 reference that must be subtracted from the total column to obtain the tropospheric column. Those intermediate parameters are assembled to derive the final column data products: the total and the tropospheric column data:

$$VCD_{tropo} = (SCD - AMF_{strato} * VCD_{strato}) / AMF_{tropo}$$

$$VCD_{tot} = VCD_{tropo} + VCD_{strato}$$

The GDP 4.9 processor is coherent with processor GDP 4.8 operational MetOp-A/B data, with only few changes in the DOAS module, but no changes in the cloud or AMF modules. Details of the DOAS fitting are summarized in table B.1. A few adaptations have been made to account for specific GOME-2C features, such as accounting for the different GOME-2/FM2 slit function, including a pseudo-cross section to account for changes in spectral resolution, and changing of the fitting window, from 425-450nm to 430.2–465nm. The last two are needed because of a strong resolution changes over the orbit and L1 calibration issues for GOME-2C (see ATBD, 2019).

Table B.1: Summary of DOAS settings for GOME-2A and GOME-2B (GDP 4.8) and GOME-2C (GDP 4.9)

	GOME-2A and GOME-2B (GDP 4.8)
Calibration	SAO2010 (Chance&Kurucz, 2010)
Slit function	FM203(GOME-2A)/FM202(GOME-2B) from GOME-2 calibration key data (EUMETSAT, 2009)
Fitting window	425-450nm
Polynomial	Cubic (4 coefficients)
Intensity offset	linearized (inversed earth-shine)
NO_2	Vandaele et al., 2002 at 240K
O_3	Gür et al., 2005 at 221K
O_2-O_2	Greenblatt et al. (1990) recalibrated

H_20	HITRAN (Rothman et al., 2003)
Ring effect	1 additive Fraunhofer Ring spectrum
Specificities for GOME-2C (GDP 4.9)	DOAS fitting window changed to 430.2–465nm; Inclusion of a resolution pseudo cross-section in the DOAS fit; Slit function: FM201(GOME-2C) from GOME-2C calibration key data (EUMETSAT, 2018)

An end-to-end validation of critical individual components of the level-1-to-2 retrieval chain has been performed as in the past, to detect anomalies and quantify uncertainties affecting intermediate parameters but possibly cancelling each other in the final data product. This end-to-end approach consists in:

(a) an assessment of the quality of GOME-2C intermediate results, by confrontation of retrievals performed respectively on GOME-2B (and GOME-2A) spectra, on an orbit-to-orbit base, through comparisons of several months averages maps and time-series comparisons;

(b) an assessment of the geophysical validity of total/stratospheric column measurements by comparison with stratospheric column measurements provided by zenith-sky DOAS UV-visible spectrometers affiliated with the Network for the Detection of Atmospheric Composition Change (NDACC);

(c) an assessment of the validity of the GOME-2C tropospheric NO_2 column data, with respect to MAX-DOAS observations performed by BIRA-IASB and partners of the NIDFORVAL project;

(d) an assessment of the validity of the GOME-2C total NO_2 column data, with respect to PANDORA observations performed within the Pandora Global Network (PGN).

B.2. Reference data

GOME-2B and GOME-2C NO_2 VCDs are compared to correlative ground-based observations, as done in the previous Validation Report for GDP 4.8 (NO_2 ACSAF VR 2017) and routinely in the Operation Reports. These includes measurements coming from different networks/instruments.

Zenith-sky twilight DOAS UV-visible measurements from the NDACC network, mostly sensitive to stratospheric NO_2 due to their particular measurement geometry, are used to assess the GOME-2 stratospheric column from pole to pole (Lambert et al. 2004, Lambert 2006, Ionov et al. 2008, Celarier et al. 2008). For the GOME-2C period, this initial validation relies on the early delivery of provisional data by NDACC/UVVIS network affiliates. This early delivery is provided by the NRT processing facility operated by LATMOS for about 15 instruments of the SAOZ type. For other instruments, early delivery must be arranged individually with the instrument PIs (several of them continue fast data delivery initiated in 2006 in the framework of the joint ESA/EUMETSAT RAO on the Calibration and Validation of EPS/MetOp data). Results relying on early-delivery data must always be considered as preliminary. Consolidated data from all ground-based stations and with official NDACC endorsement is available via the NDACC Data Host Facility (see http://www.ndacc.org) within one year after acquisition, in accordance with NDACC Data Protocols.

MAXDOAS measurements are used to validate satellite tropospheric NO_2 columns (Brinksma et al. 2008; Celarier et al. 2008, Irie et al. 2008, Ma et al. 2013, Kanaya et al. 2014, Drosoglou et al. 2017 ; Boersma et al. 2018, Compernolle et al. 2019, Pinardi et al., in prep.). The affiliation of MAXDOAS instruments in the NDACC network is under progress, following efforts done in the NORS, QA4ECV and ESA's FRM4DOAS project to harmonize and automatize data processing. Due to instrumental failures, the number of BIRA-IASB currently operating MAXDOAS instruments is limited (for the GOME-2C received period February to July 2019, only Uccle and Reunion-Maido instruments were measuring). The comparisons have thus been extended to ground-based data collected by BIRA-IASB from different partners in the context of the S5PVT AO project NIDFORVAL (S5P NItrogen Dioxide and FORmaldehyde Validation using NDACC and complementary FTIR and UV-Vis DOAS ground-based remote sensing data). This ESA AO project aims at creating and collecting ground-based datasets from NDACC and complementary networks, to be used in the validation of TROPOMI data.

Pandora spectrometers measuring in direct-sun mode are sensitive to the total NO_2 columns. The light travels through the whole atmosphere and the measurement in this geometry is equally sensitive to both troposphere and stratosphere. These instruments provide accurate total column measurements with a minimum of a-priori assumptions. Standardized Pandora sun-photometers (Herman et al., 2009; Tzortziou et al., 2013; Herman et al., 2019) are nowadays the largest contributor of direct-sun total NO_2 column data, encouraged by their network operation into the Pandonia Global Network (PGN, https://www.pandonia-global-network.org). Past validation of GOME-2 A/B data with Pandora (NO_2 ACSAF VR 2017; Pinardi et al., in prep.) is here extended to GOME-2C with recent PGN measurements gathered in a demonstration phase within the NIDFORVAL project, and now available in NRT through the PGN archive, mirrored at EVDC, and used in the MPC CalVal VDAF webserver (http://mpc-vdaf-server.tropomi.eu/no2) for the routine validation of S5p total NO_2 columns.

C. VERIFICATION OF INDIVIDUAL COMPONENTS OF THE METOP-C GOME-2 PROCESSING CHAIN: METOP-C AGAINST METOP-B

C.1. Verification of Slant Column Density

To test the quality of the DOAS NO_2 slant column fit on GOME2-C spectra, GDP has been used to retrieve NO_2 slant column amounts from spectra recorded along a single orbit of GOME-2 Metop-C (orbit #1535, February 23, 2019), and of GOME-2 Metop-B in 2019 (orbit #33378, February 23, 2019). Current version of GDP product for GOME-2 Metop-B and -C are 4.8 and 4.9, respectively.

The NO_2 slant column from two sensors are highly consistent (Figure C.1.1). Compared to the Metop-B, GOME-2 Metop-C NO2 columns are slightly larger for most of regions, with relatively smaller standard deviation. Scatter of the slant columns from GOME-2B is 10% higher than GOME-2C.

The fitting residual from GOME-2C is systematic lower than residual from GOME-2B, and the residual from GOME-2B shows strong latitude-dependence, high in the southern and low in the northern hemisphere, but not obvious for GOME-2C.

Please note that the coverage of a Metop-B and Metop-C orbit is not exactly the same, and overpass time in the same location is different between two sensors as well. The NO_2 columns have large temporal and spatial variation over the polluted regions.

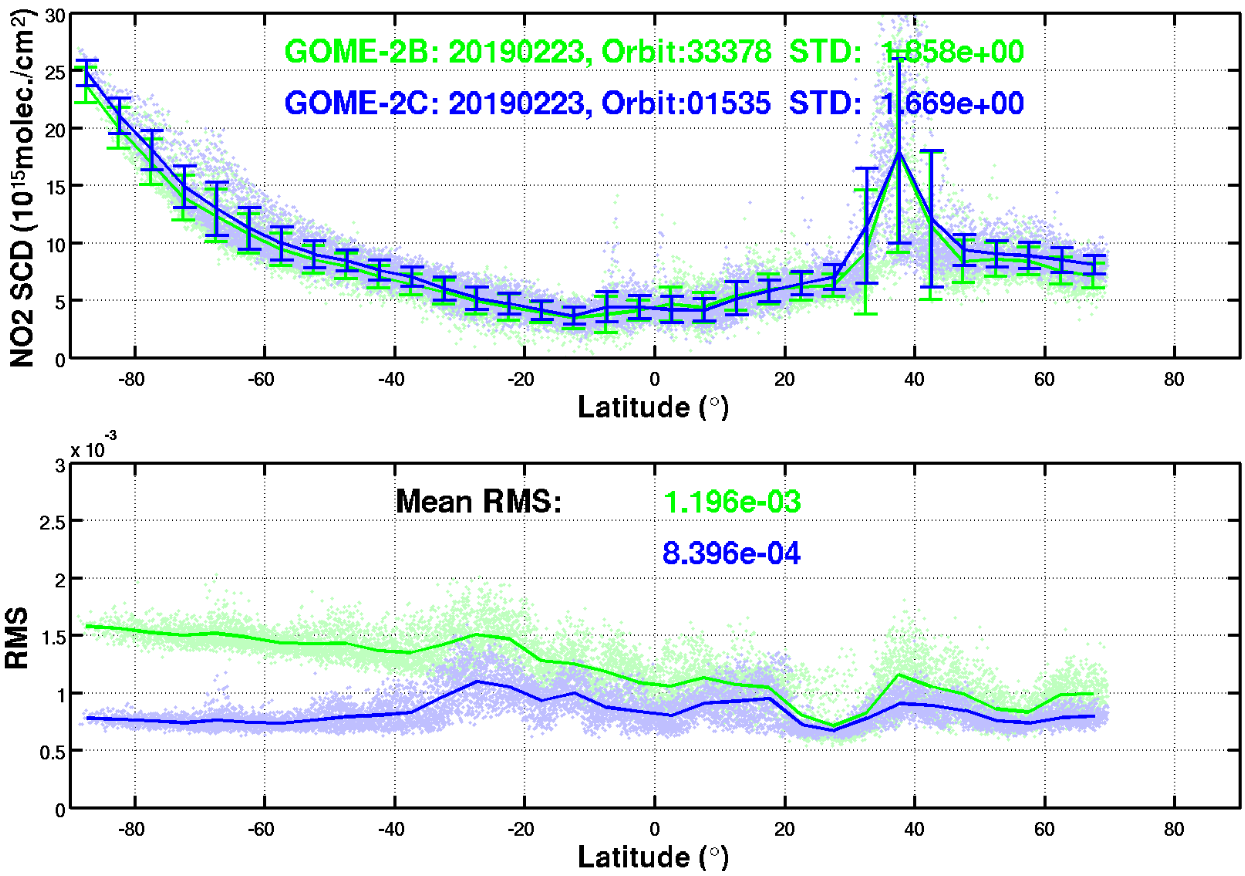

Figure C.1.1: NO_2 retrievals for one orbit of GOME-2 on METOP-B (green, 23/02/2019, orbit nb. 33378) and METOP-C (blue, 23/02/2019, orbit nb. 1535) in 2019. Dots are individual measurements; lines are averages within 5° latitude-bands. First panel: slant columns and standard deviation of the slant columns within the 5° latitude-bands (STD), second panel: residuals of the fit (RMS).

The estimation of the precision of the NO_2 slant column densities is derived from a statistical analysis of the GOME-2 measurements in the clean tropical Pacific region (20°S–20°N; 150°E–150°W). This region is divided into small boxes (2°×2°), and from the variation of the NO_2 columns within each box, an estimate of the slant column precision can be made. (Note that the variability of the air mass factors within the boxes is small, and is taken into account by scaling the slant columns with an appropriate geometrical air mass factor). The deviation of each GOME-2 measurement from the corresponding box mean value is calculated on a daily basis. The slant column error is then derived from the distribution of the slant column deviations, as shown in Fig. C.1.2. for GOME-2B in February 2013 and February 2019, and GOME-2C in February 2019. The distribution has a Gaussian shape. The width of the Gaussian is about 0.68, 0.72 and 0.60 × 10^{15} molec/cm^2 for above three cases, respectively, and the corresponding slant column error (≈ 0.42 × FWHM) is 0.29, 0.30 and 0.25 × 10^{15} molec/cm^2. The slant column error for GOME-2C is about 20% better than for GOME-B, and error for GOME-2B is slightly increased from 2013 to 2019, due to the instrumental degradation.

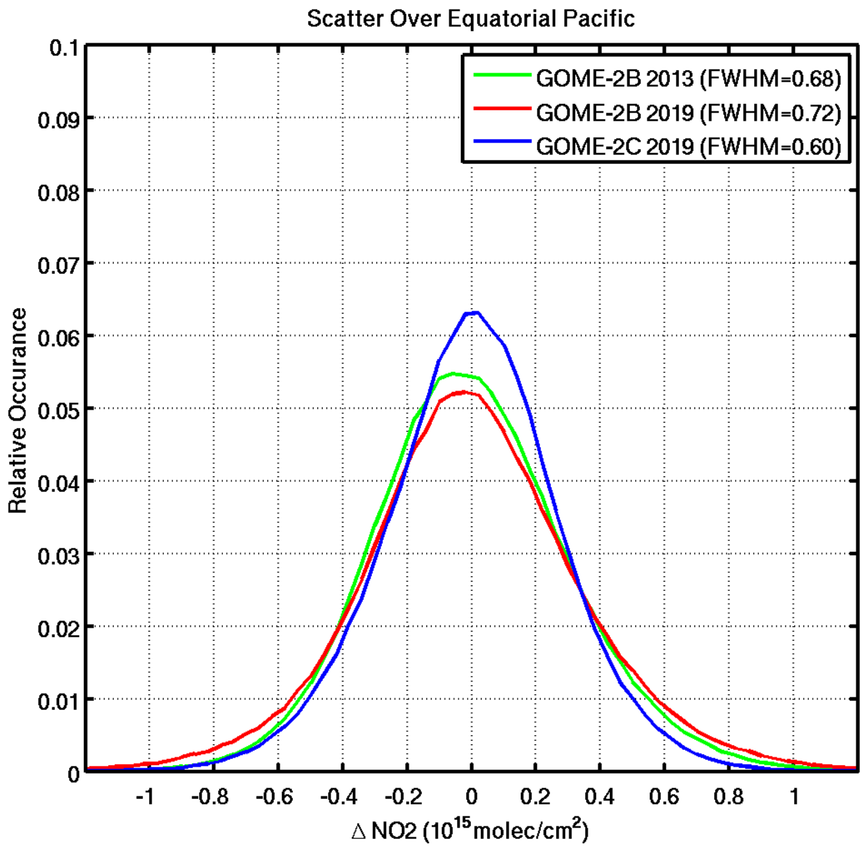

Figure C.1.2: Distribution of NO_2 vertical columns over a clean region at the equatorial Pacific (5°S-5°N, 150°E-150°W) for GOME-2B in February 2013 and February 2019, and for GOME-2C in February 2019. Geometric air mass factor was applied, and only forward scans were included. All curves were normalised to have unit area and centred at 0. See text for details on the different instruments and periods.

The averaged maps (Figure C.1.3) show prefect agreement on the NO_2 slant column distribution between GOME-2B and GOME-2C, only slightly difference over land (Figure C.1.4), GOME-2C bias high over land and high latitude regions.

Fitting residual (RMS) shows systematic higher level of noise for GOME-2B than for GOME-2C (Figure C.1.3). GOME-2B fitting residual has strongly latitude dependence, high in Southern Hemisphere and low in Northern Hemisphere, which is not the case for GOME-2C. This is probably due to the calibration issue in the GOME-2B L1b data, and to the inclusion for GOME-2C analysis of a pseudo cross-section to take into account the changes in resolution along the orbits. The GOME-2C fitting residual shows slightly higher noise over 30°S-30°N latitudes.

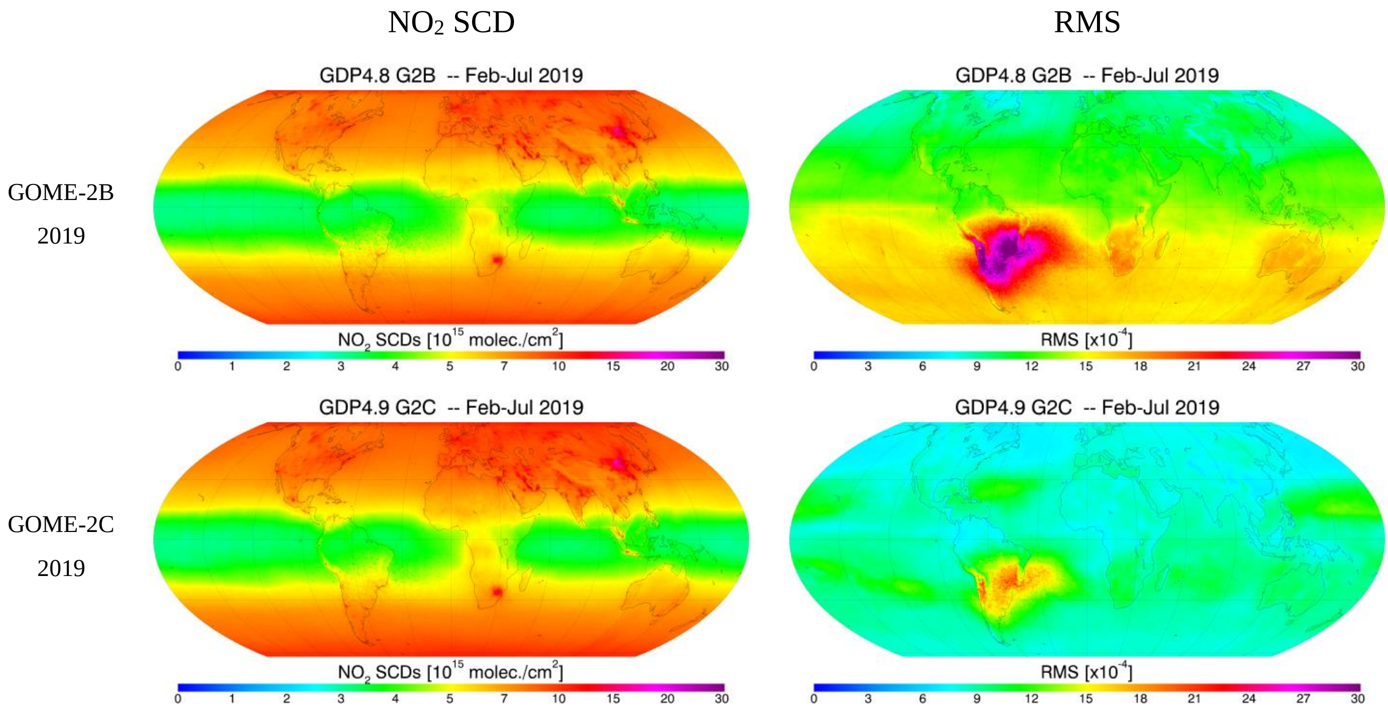

Table C.1.3: Maps of averaged slant columns, fitting residuals from February to July 2019, obtained from GDP 4.8 GOME-2B and GDP4.9 GOME-2C products.

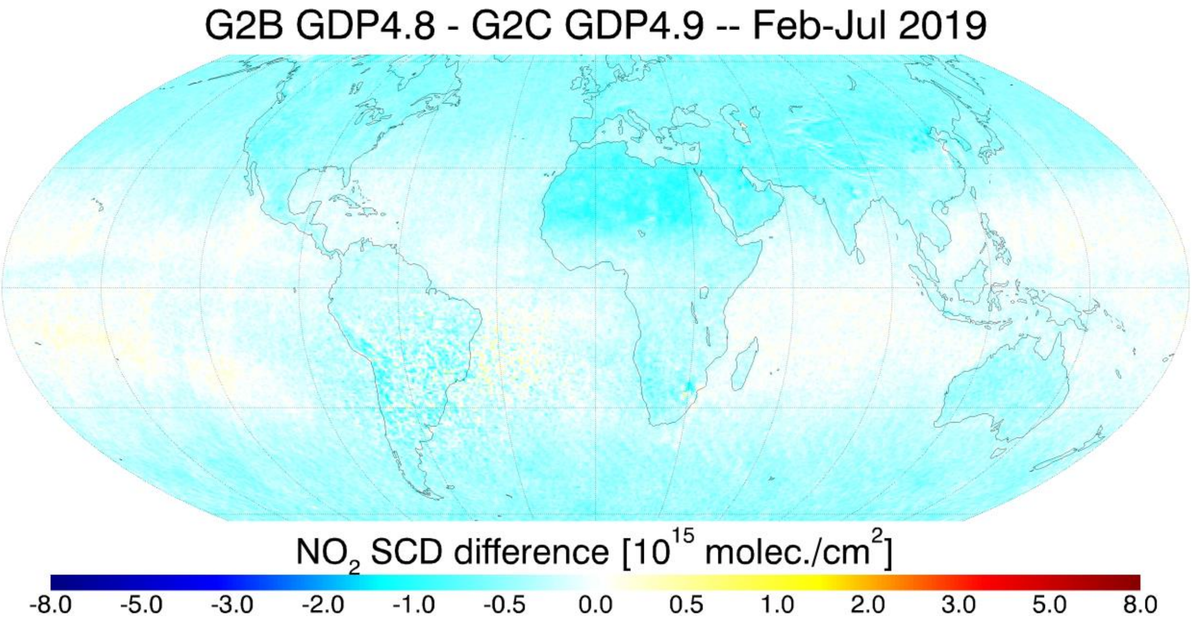

Figure C.1.4: Map of averaged slant column density differences between GOME-2B GDP4.8 and GOME-2C GDP4.9, obtained from February to July 2019.

C.2 Verification of Stratospheric correction

The GDP 4.9 GOME-2C stratospheric columns are compared to GDP 4.8 GOME-2B maps averaged from February to July 2013 in Figure C.2.1.

The systematic bias in the total NO_2 slant columns is mostly transferred into the stratospheric correction. The GOME-2B stratospheric columns are globally smaller than GOME-2C, with a latitudinal structure with smaller differences around the equator and an increase over higher latitudes (0.5~1.010^{15} molec./cm²).

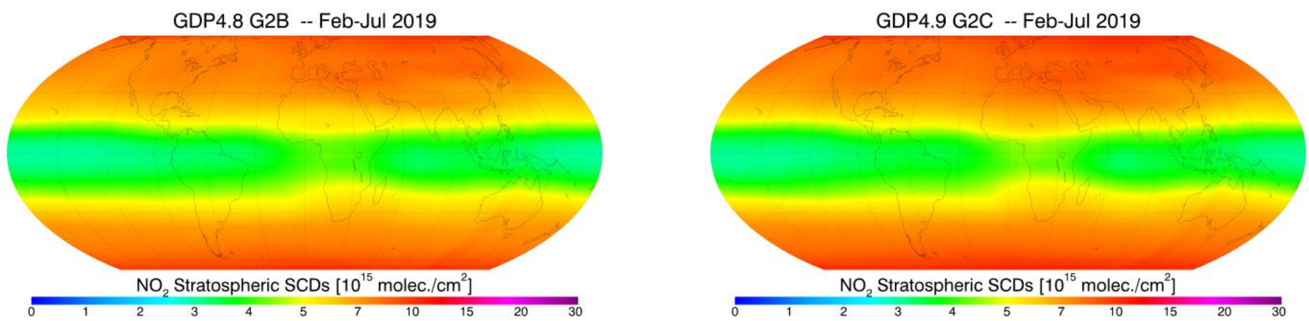

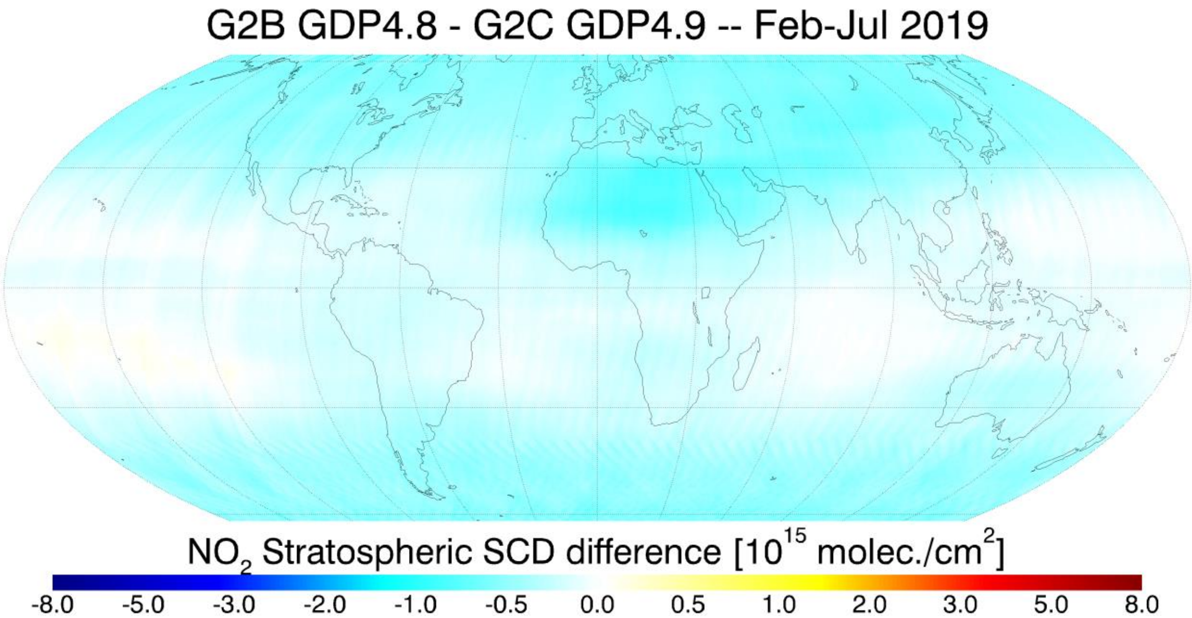

Figure C.2.1: Maps of averaged stratospheric correction, obtained from GDP4.8 on GOME-2B (top-left) and GDP4.9 on GOME-2B (top-right) measurements from February to July 2019, and their differences (bottom).

C.3 Verification of Tropospheric Vertical Column Density

This section concentrates on the verification of the tropospheric vertical column densities. Figure C.3.1 and C.3.2 illustrate the status of the comparisons between GDP4.8 applied to GOME-2B and GDP4.9 applied to GOME-2C. For the verification, the pixels with intensity-weighted cloud fraction > 50% and surface albedo > 0.3 are discard to control the quality of the retrieved data.

Good agreement between GOME-2B and GOME-2C is found for both tropospheric vertical column and tropospheric air mass factor. The GOME-2B data over 50ºS-60ºS and 25ºN-30ºN for orbit 33378 is missing (Figure C.3.1) because of the complete cloud coverage, and GOME-2C only have few valid measurements as well.

From the global average maps (Figure C.3.2) similar result as those on one orbit are found: relative good agreement between GOME-2B and GOME-2C datasets. However, there is an obvious bias over 30ºS-0º latitudes, which is not found in the slant column density, the stratospheric correction or the tropospheric air mass factor. Part of it is related to the STS algorithm. The high bias in the total NO_2 columns from GOME-2C over land is causing issues with the STS algorithm (e.g. due to the masking of polluted areas mainly over land), and has an impact on the trop. NO_2 columns (i.e. the total NO_2 bias over land might not be "fully transferred" to the stratospheric column). This is visible in the first panel of Figure C3.3, presenting the difference in tropospheric NO_2 between GOME-2B and GOME-2C, where a bias over land, but not over ocean, is present. The bias in tropospheric SCD is up to ~0.25 x 10^{15} molec/cm².

Another part of the reason is related to the data selection criteria. Differences in the tropospheric NO_2 column residual (slant column minus stratospheric correction) using different criteria are compared in Figure C.3.3. The conditions for the data selection includes valid SCD, cloud-free (intensity-weighted cloud fraction < 50%), snow-free (surface albedo < 0.3), and valid tropospheric air mass factor. Figure C.3.3 clearly shows that the main factor of the discrepancy is due to the filtering on the valid tropospheric air mass factor, which leads to a bias such as the one in tropospheric NO_2 columns between GOME-2B and GOME-2C.

Further investigation find that calculation of tropospheric air mass is terminated when the error of the slant column from DOAS fitting > 50%. This situation appears more often in GOME-2B than in GOME-2C, due to better spectral quality for GOME-2C, and resulting in lower fitting residual for NO_2 retrieval, especially over Southern Hemisphere (Figure C.1.3). Cutting-off the retrieval for the measurements with the large SCD error leads to an overestimation in the GOME-2B average map.

Based on the monthly averaged maps (gridded at 0.5°×0.5°) from February to July 2019, the difference in tropospheric vertical column density between GOME-2B and GOME-2C is ~32% (between 70°S and 70°N, and excluding the SAA regions) for pixels with VCD values exceeding 0.5×10^{15} molecules/cm^2. If only pixels with VCD larger than 2.5×10^{15} molecules/cm^2 are considered, the average difference between GOME-2B and GOME-2C is within 17%. It meets the optimal accuracy of requirement for tropospheric NO_2 (20%).

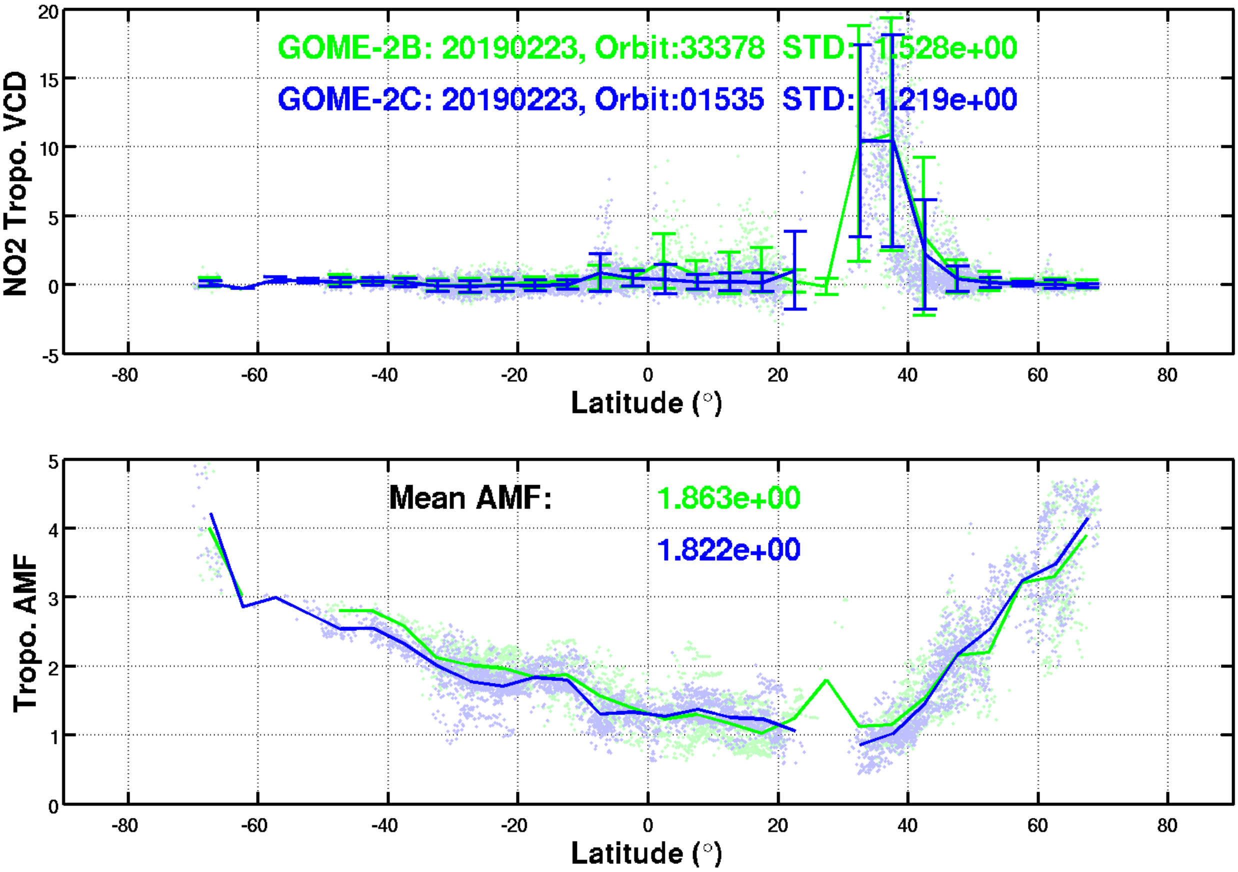

Figure C.3.1: NO_2 retrievals for one orbit of GOME-2 on METOP-B (green, 23/02/2019, orbit nb. 33378) and METOP-C (blue, 23/02/2019, orbit nb. 1535) in 2019. Dots are individual measurements; lines are averages within 5° latitude-bands. First panel: slant columns and standard deviation of the slant columns within the 5° latitude-bands (STD), second panel: residuals of the fit (RMS). Only the valid NO_2 retrieval with intensity-weighted cloud fraction less than 50% and surface albedo less than 0.3 are used.

Tropospheric NO_2 VCD   Tropospheric AMF

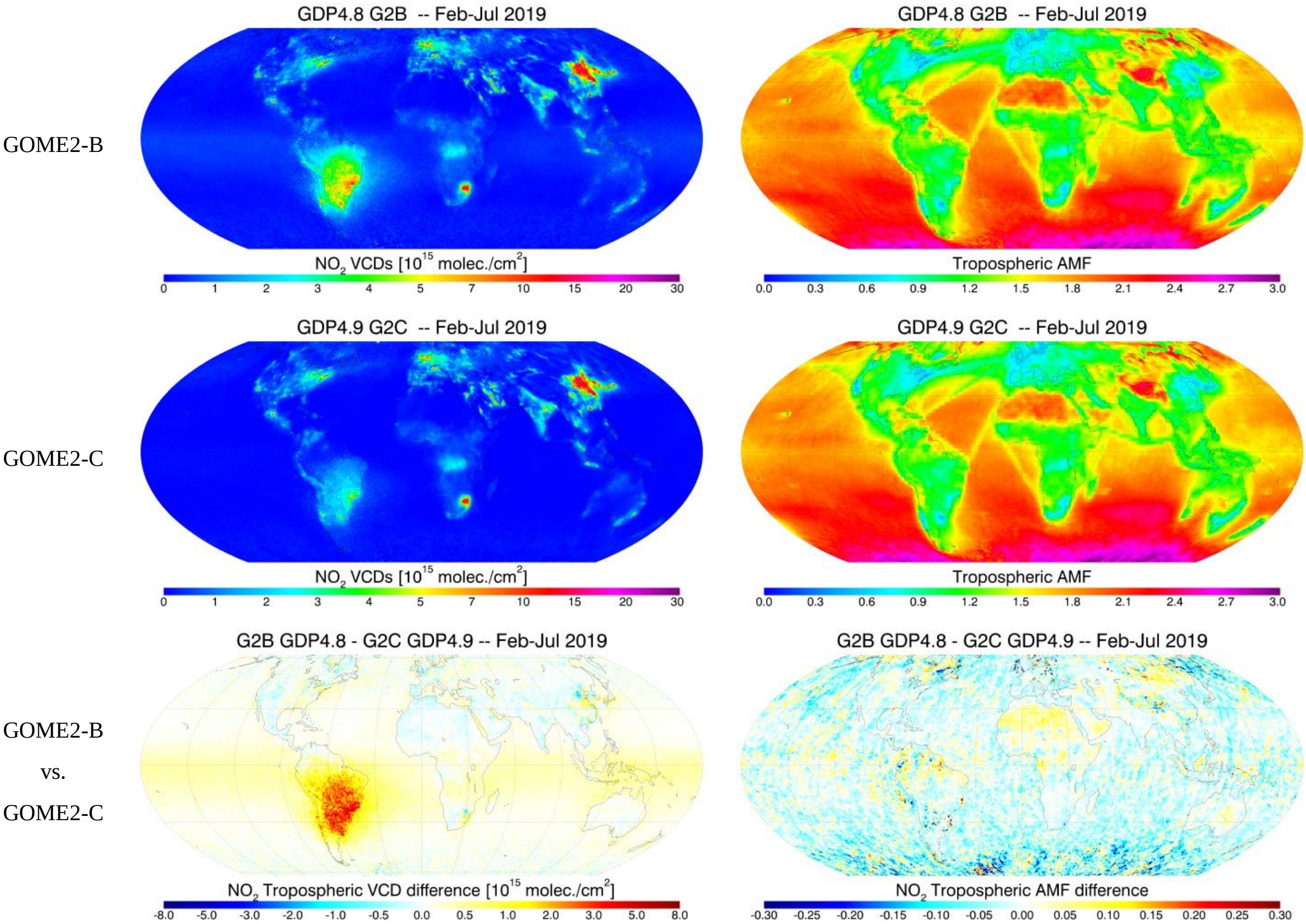

Figure C.3.2: Maps of averaged tropospheric vertical columns and tropospheric air mass factor, obtained from GDP 4.8 GOME-2B and GDP4.9 GOME-2C cloud- and snow-free (intensity-weighted cloud fraction < 50% and surface albedo < 0.3) measurements from February to July 2019, and their differences.

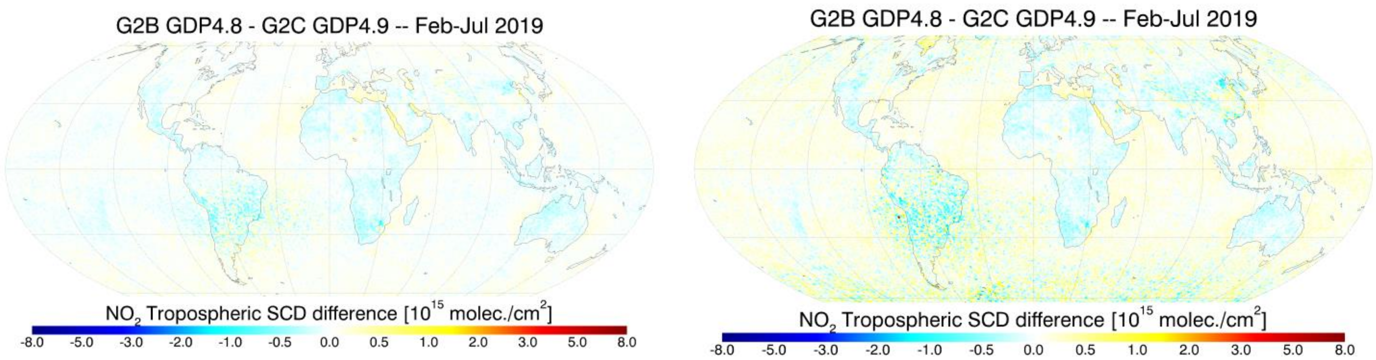

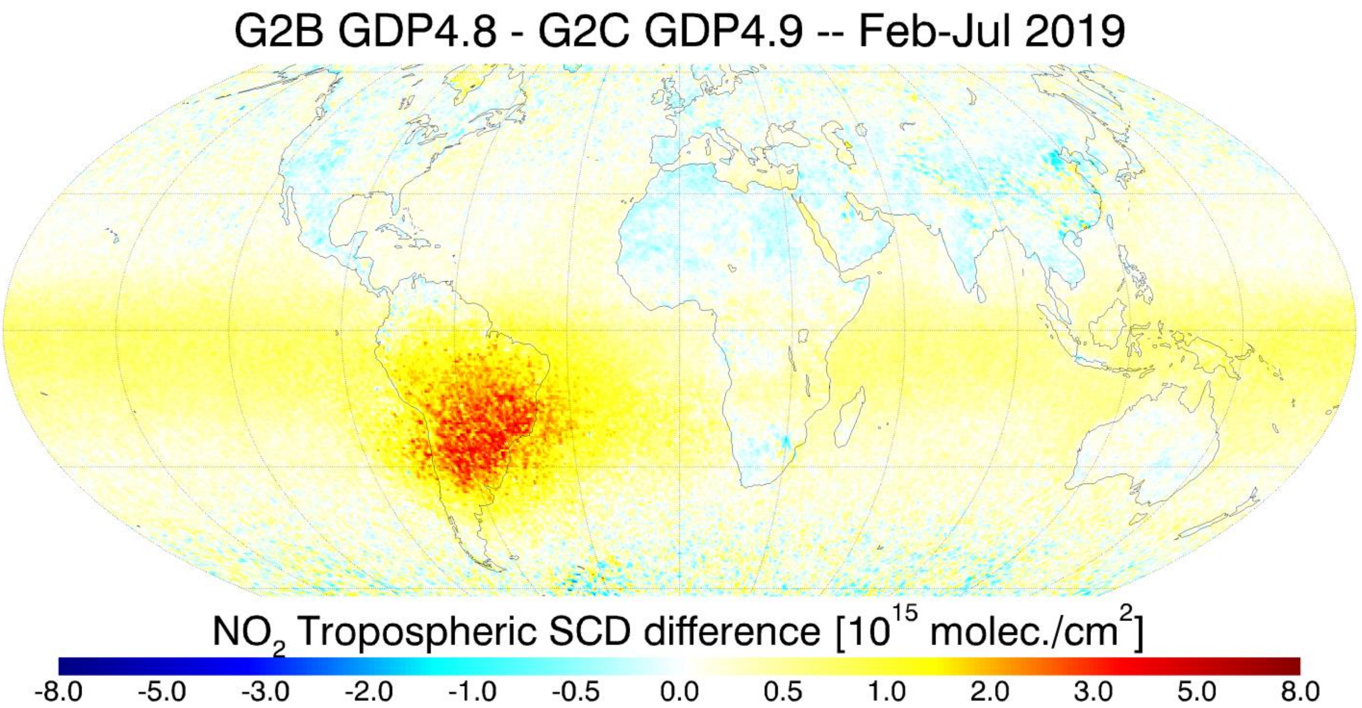

Figure C.3.3: Maps of the differences in tropospheric NO2 residual between GDP 4.8 GOME-2B and GDPO4.9 GOME-2C data sets from February to July 2019. Top-left: valid SCD retrieval; top-right: valid SCD retrieval with intensity-weighted cloud fraction less than 50% and surface albedo less than 0.3; bottom: valid SCD retrieval, intensity-weighted cloud fraction < 50%, surface albedo < 0.3 and valid tropospheric air mass factor.

C.4 Verification of Vertical Column Density

To verify the GDP 4.9 GOME-2C total vertical columns against GDP 4.8 GOME-2B product, the results of two datasets are compared for the average from February to July 2019 in Figure C.4.1. Based on the discussion in the previous sections, the positive GOME-2C bias over land and high latitudes is mainly due to the difference in the slant column density between two sensors, and the difference in the criteria of data selection lead to the positive bias between 30°S and 0° in the average map.

Based on the monthly averaged data (gridded at 0.5°×0.5°) between 70°S and 70°N, obtained from February to July 2019, the difference in total NO_2 vertical column density between GOME-2B and GOME-2C is 2.5×10^{14} molecules/cm^2, which reach the optimal accuracy ($1\text{-}3\times10^{14}$) of the requirement.

GOME-2B GOME-2C

Total VCD

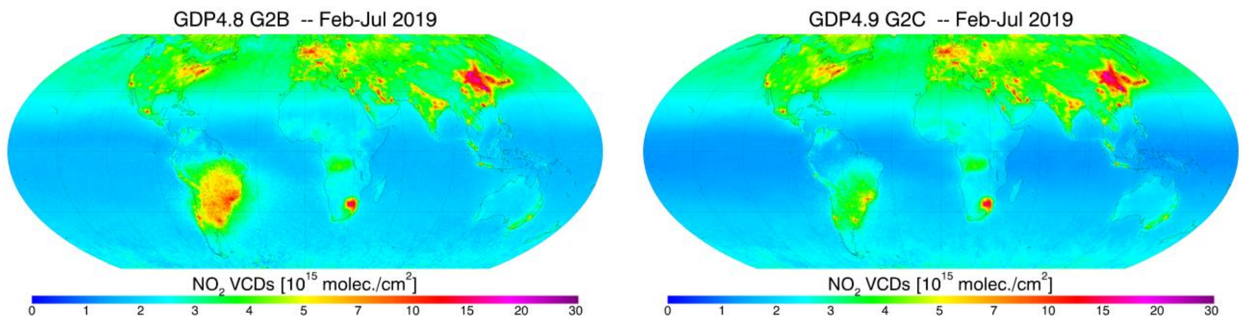

GOME-2B

vs.

GOME-2C

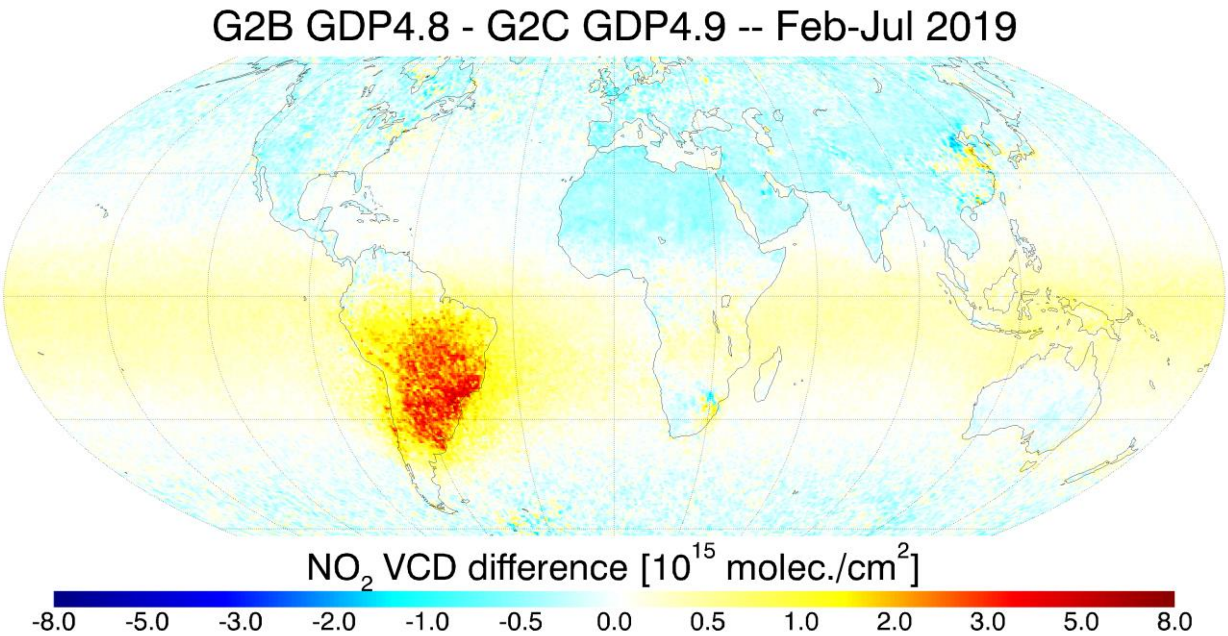

Figure C.4.1: Maps of total NO_2 column density, obtained from GDP4.8 on GOME-2B (top-left) and GDP4.9 on GOME-2C (top-right) measurements from February to July 2019, and their differences (bottom), only the measurements with intensity-weighted cloud fraction < 50%, surface albedo < 0.3 and valid tropospheric NO_2 retrievals are used in the analysis.

C.5. Individual components above three sites

In order to conclude this section, time-series of the different contributions of the operational processing chain of both Metop-A, Metop-B and Metop-C are presented at 3 BIRA-IASB MAXDOAS stations, historically used for the tropospheric NO_2 data validation as representative of different NO_2 levels, and partly used in Section D.2. These are the remote OHP area (South of France), the urban Uccle area (Belgium) and the sub-urban Xianghe case (China). Monthly mean averages are performed for the daily closest cloud free pixels within 100km around the station.

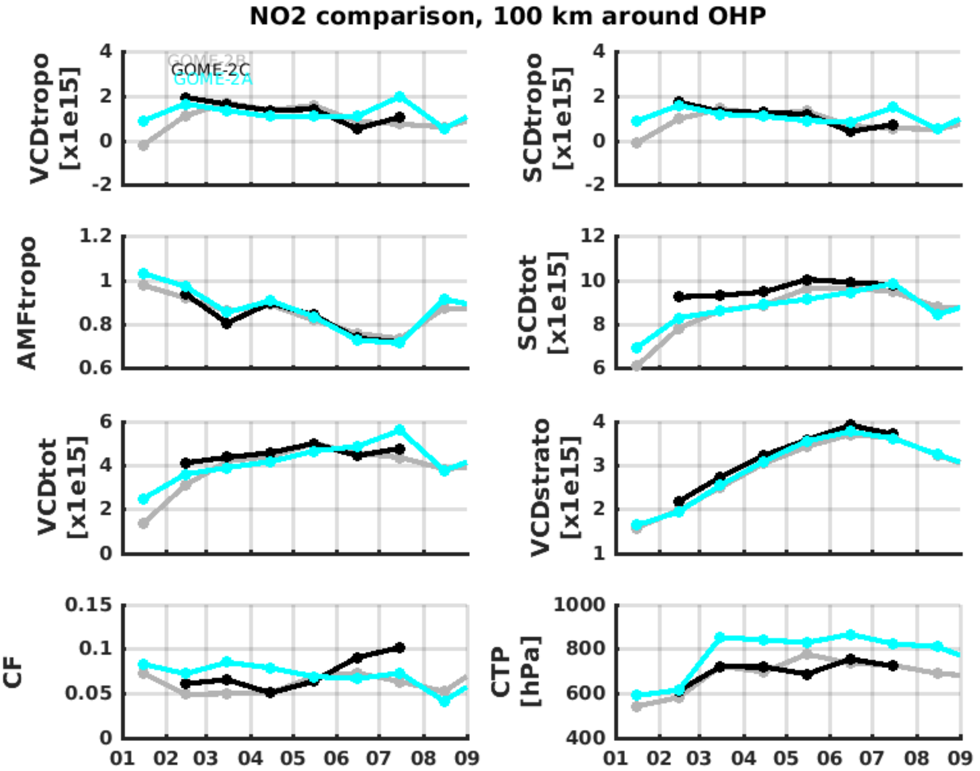

Figure C.5.1 End-to-end comparison between GOME-2C (in black), GOME-2B (in grey) and GOME-2A (cyan) monthly mean averages in a region of 100 km around OHP. The different contributions of the NO2 retrieval are investigated: tropospheric VCD, total VCD, total SCD, tropospheric SCD, stratospheric VCD, tropospheric AMF and cloud fraction CF and cloud top pressure (CTP).

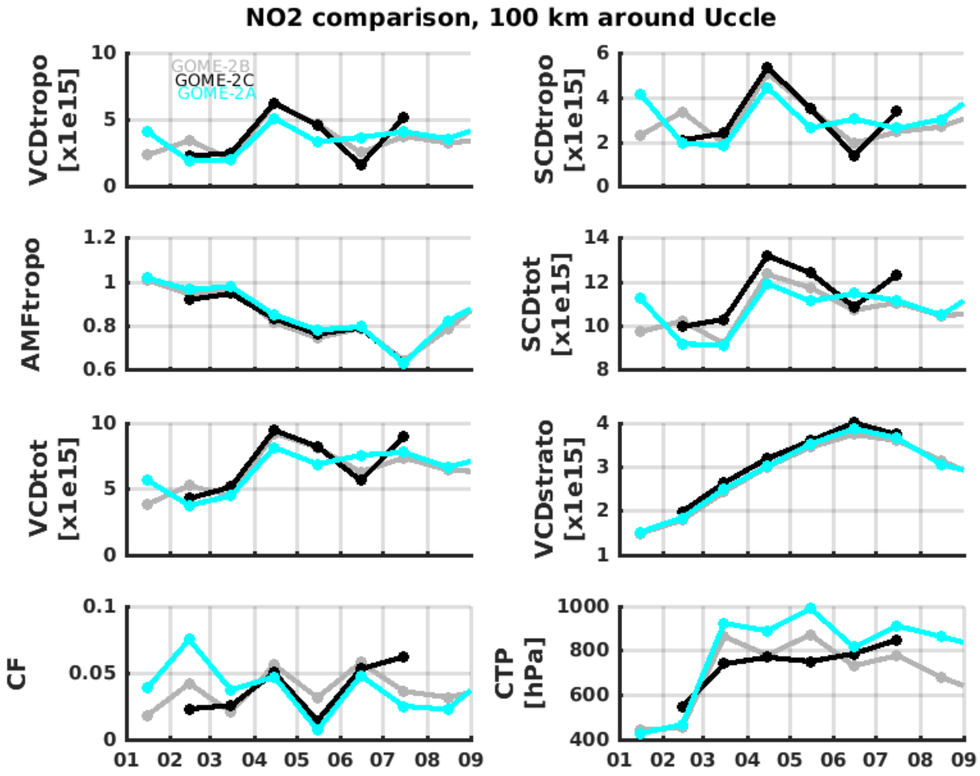

Figure C.5.2 As C.5.1 but for Uccle station.

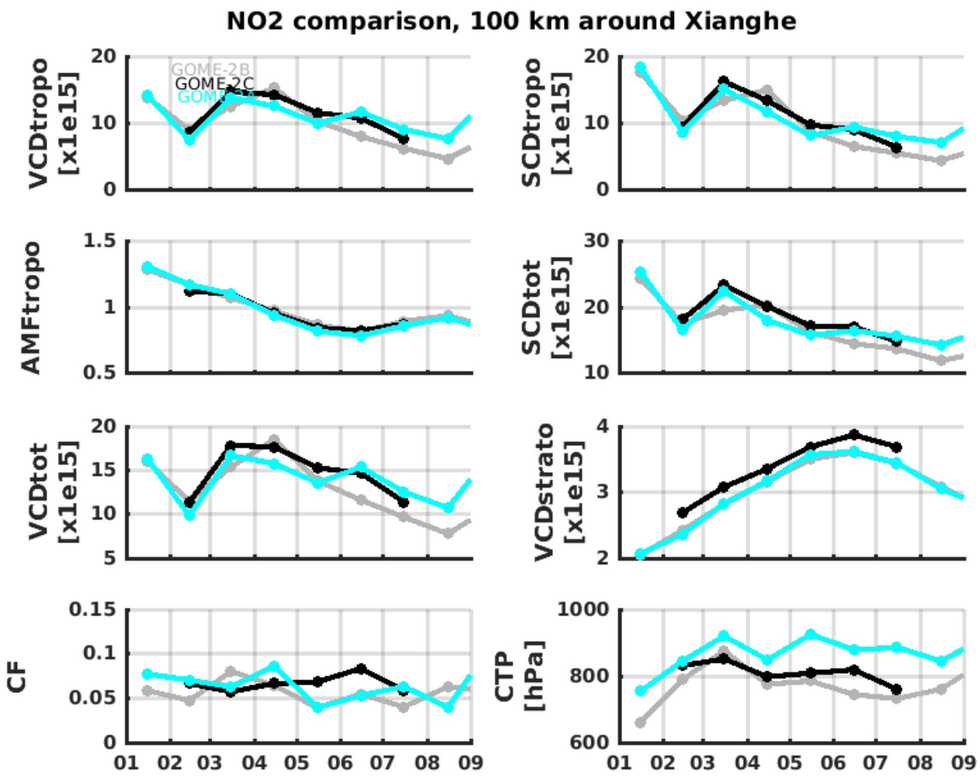

Figure C.5.3 As C.5.1 but for Xianghe station.

Figures C.5.1 to C.5.3 present the GOME-2C temporal evolution, which is generally in good agreement with the GOME-2B evolution, for the different component of the retrieval and for the different pollution conditions. Slightly larger differences appear for GOME-2A, probably due to degradation issues and smaller pixels due to the swatch change. Tropospheric AMF are very coherent for the 3 instruments over the 3 sites. Cloud properties can be quite variables, which is partially to be expected, due to the different overpasses and orbit configurations, especially for GOME-2A (reduced swath). The larger GOME-2C slant columns (and stratospheric column) wrt GOME-2B over land pointed out in the previous sections, is also observed in the time-series over these stations, partially also affecting the next steps of the NO_2 retrieval (the slant column, the SCDtropo, VCDstrato, VCDtropo and VCDtot).

D. EVALUATION OF THE NO_2 COLUMN DATA PRODUCTS

D.1. Stratospheric Vertical Column

D.1.1 Comparison against ground-based zenith-sky twilight DOAS data

This chapter reports on comparisons of GOME-2C GDP 4.9 stratospheric NO_2 column data against ground-based reference measurements acquired routinely at twilight by zenith-sky looking UV-visible spectrometers (ZLS-DOAS). All considered ZLS-DOAS instruments perform network operation in the context of NDACC, with due certification of their measurement protocol and quality control of their data. NDACC stations having provided data for this initial GOME-2C validation study are highlighted in red in Figure D.1.1. They consist mainly in SAOZ stations from where data are processed in near-real-time and collected through the CNRS LATMOS central processing facility. In several graphs, for reference, comparison results are shown also for both the operational GOME-2A GDP 4.8 and GOME-2B GDP 4.8 stratospheric NO_2 data. Due to the photochemical diurnal cycle of the nitrogen oxides family associated with changes in solar illumination, a bias appears between twilight measurements acquired by definition between 86° and 91° SZA, and GOME-2 measurements acquired at a solar local time linked to the orbit of the MetOp platforms: usually in the mid-morning, but also at larger SZAs in polar areas, and at various SZAs in case of multiple daily overpasses during polar day. To avoid this bias, in this study only twilight GOME-2 data (hereafter beyond 75° SZA) are to be considered during polar day, and only sunrise ZLS-DOAS measurements (blue curves) are to be considered elsewhere (at low and middle latitudes sunrise NO_2 differ from mid-morning NO_2 by only a few 10^{14} molec.cm^{-2}). At twilight the zenith-sky viewing geometry becomes sensitive mainly to stratospheric absorbers like NO_2, which makes it particularly suitable for stratospheric validations.

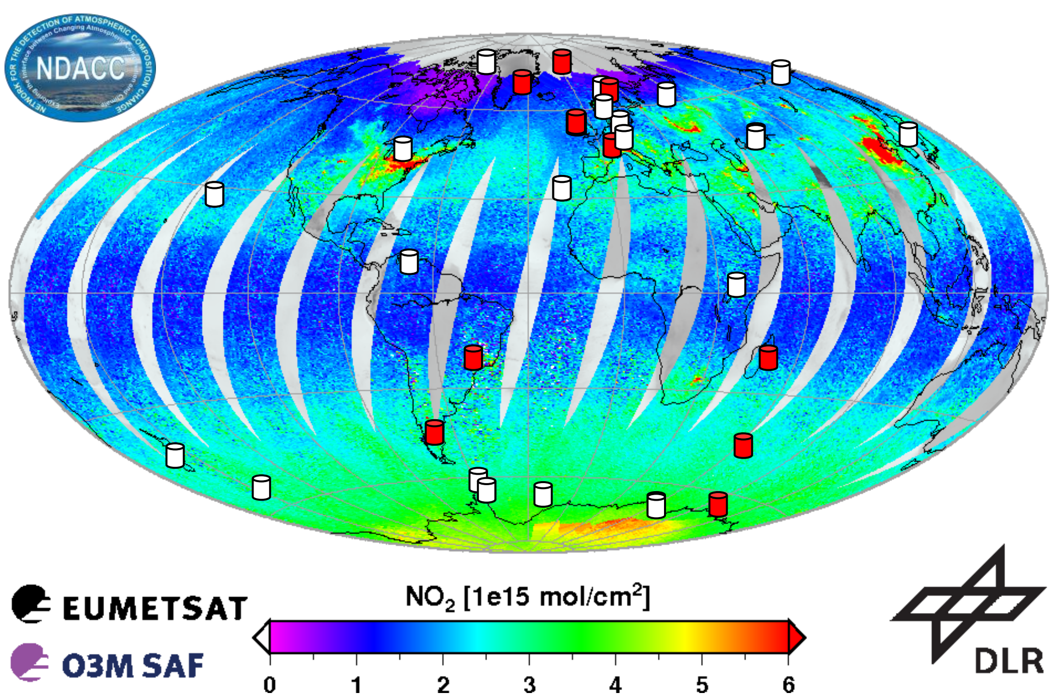

Figure D.1.1 Geographical distribution of NDACC UVVIS (SAOZ) spectrometers measuring the NO_2 total column at twilight. Stations having provided data for this GOME-2C validation study are highlighted in red. Stations are displayed on top of the global NO_2 field measured by GOME-2A on February 10, 2011.

Hereafter comparison results are reported at illustrative stations from the Arctic (Section D.1.1.1) to the Antarctic (D.1.1.5), and summarized in Section D.1.1.6, at 14 stations representative of the following atmospheric states and observational conditions:

- Southern middle latitude stations, combining negligible tropospheric pollution, easy-to-handle diurnal cycle of stratospheric NO_2 (sunrise values close to mid-morning values), and large NO_2 SNR.
- Clean Northern middle latitude sites surrounded by large polluted areas, where pollution episodes have been filtered out for fractional cloud covers below 25%.
- Polar stations, with polar day exhibiting a particular diurnal cycle sampled several times a day by GOME-2, and polar wintertime with low NO_2 columns and SNR and large relative variability.
- Tropical stations, with low NO_2 columns observed under small SZA, which result in poorer SNR.

D.1.1.1 Stratospheric NO_2 column over the Arctic

Figures D1.2 to D1.4 present comparisons at three NDACC stations located in the Arctic: Ny-Ålesund on Spitsbergen, Scoresbysund in Greenland, and Sodankylä in Finland. Statistics on absolute differences presented in the bottom plots are based on monthly medians and interpercentile values rather than means and standard deviations, to avoid unwanted overweight of exceptional outliers. At all stations GOME-2C GDP 4.9 and NDACC ZLS-DOAS SAOZ instruments capture similarly the seasonal cycle of stratospheric NO_2, as well as monthly and day-to-day changes in stratospheric NO_2. Quantitatively, outside of polar day conditions, GOME-2C agrees with ground-based measurements by about a few 10^{14} molec.cm^{-2}, that is, within the uncertainty bar of the comparison method. During polar day results differences remain at similar levels at Scoresbysund and Sodankylä, but at Ny-Ålesund the negative bias of a few 10^{14} molec.cm^{-2} increases to a more significant value of about -1 10^{15} molec.cm^{-2}. Since this increasing bias might be due to uncertainties associated with the SAOZ RT processing and/or non-perfect correction of diurnal cycle effects, this validation analysis should be revisited at a later stage once V3 reprocessing of the SAOZ data becomes available, and also with improved diurnal cycle correction tailored to the GOME-2C observational parameters (so far all GOME-2 data are corrected similarly, without distinction of the platform and thus effective solar local time). A clue of the need to revisit the diurnal correction for GOME-2C is provided by Figure D.1.5: the dependence on SZA exhibits a marked structure, while after correction of the photochemical effects the dependence on SZA should be more or less flat. Moreover, the photochemical correction used here working at best for GOME-2 data acquitted at the largest SZAs on the orbit a better agreement to within $2\text{-}5\cdot10^{14}$ molec.cm^{-2} is obtained if we consider only measurements coincident in time, that is at twilight SZAs. The agreement is also good in the 55°-70° SZA range, where the photochemical correction works also well.

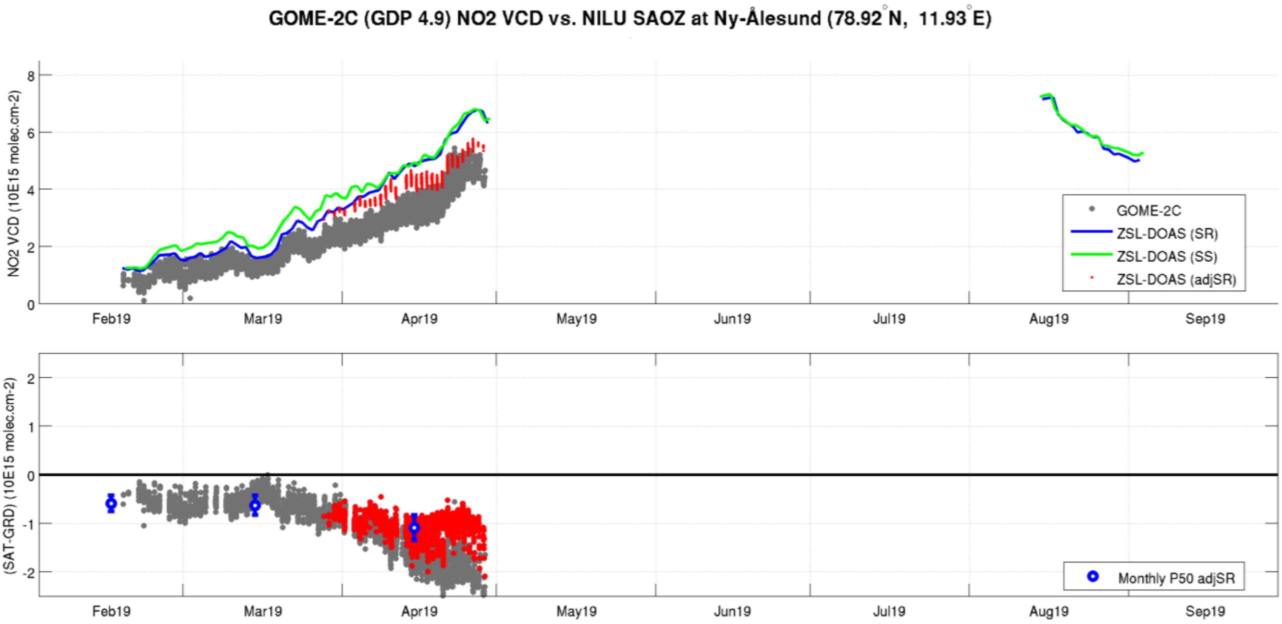

GOME2 NRT_OFL GDP 4.9 NO2 vertical column 5795 pixels in 71 days (17/02/2019 - 28/04/2019)				Ny-Ålesund (78.92°N, 11.93°E) NILU SAOZ (NC), source: LATMOS_RT 170 meas. in 91 days (17/02/2019 - 03/09/2019)				Method: zovp pixels (all CF) vs. Twilights Global agreement: -0.9 ± 0.4 (10^{15}mol.cm^{-2}) Linear drift: NaN*t (10^{15}mol.cm^{-2}/year) , ϕ = NaN				
	January	February	March	April	May	June	July	August	September	October	November	December
2019	-	-0.6 ± 0.2	-0.6 ± 0.2	-1.1 ± 0.3	-	-	-	-	-	-	-	-

Figure D.1.2 Comparison of NO_2 total column measured at the NDACC station of the Ny-Ålesund (Spitsbergen) by GOME-2-C (GDP 4.9) and by the SAOZ UVVIS spectrometer operated by NILU (LATMOS RT processing). Top panel: total NO_2 data; bottom panel: difference between GOME-2C and SAOZ total NO_2 data. Red dots indicate comparison results after correction for the daily photochemical cycle during polar day. Monthly medians (P50, blue open dots) and corresponding 68% interpercentile (error bars) based on all GOME-2C data and on sunrise (blue curve) SAOZ data only.

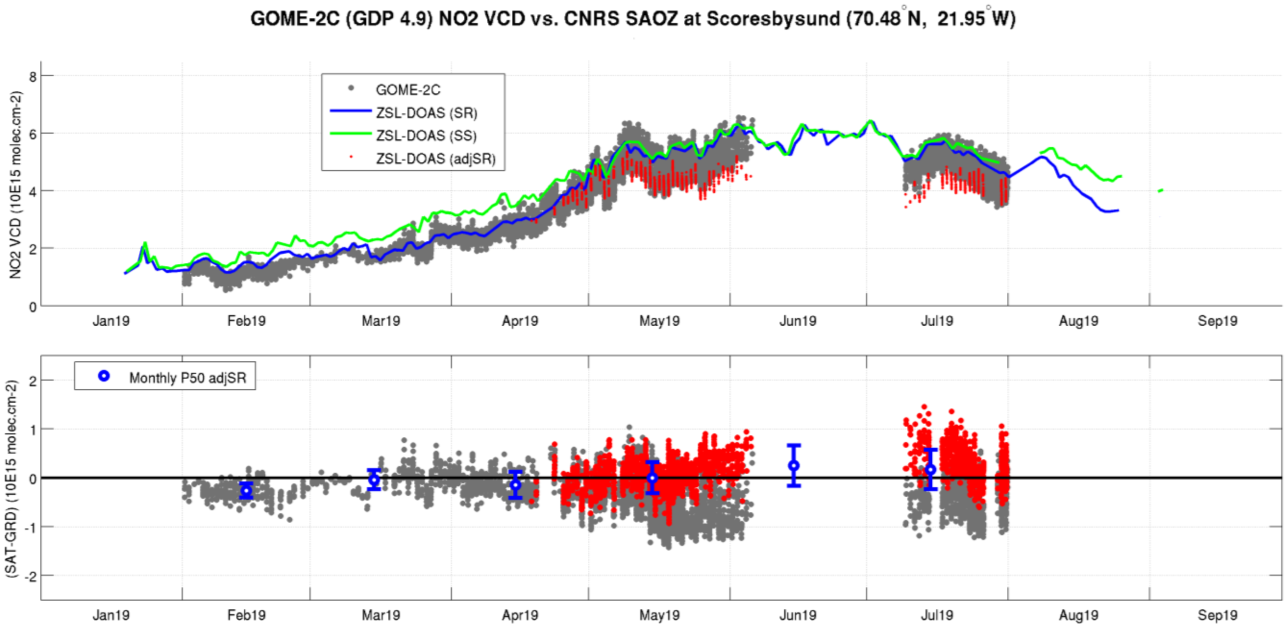

GOME2 NRT_OFL GDP 4.9 NO2 vertical column 7825 pixels in 148 days (01/02/2019 - 31/07/2019)			Scoresbysund (70.48°N, 21.95°W) CNRS SAOZ (CP200_NMOS1024), source: LATMOS_RT 419 meas. in 224 days (01/11/2018 - 03/09/2019)				Method: zovp pixels (all CF) vs. Twilights Global agreement: -0.0 ± 0.3 (10^{15}mol.cm^{-2}) Linear drift: NaN*t (10^{15}mol.cm^{-2}/year), ϕ = NaN				
	January	February	March	April	May	June	July	August	September	October	November	December
2019	-	-0.3 ± 0.1	-0.0 ± 0.2	-0.1 ± 0.3	-0.0 ± 0.3	0.2 ± 0.4	0.2 ± 0.4	-	-	-	-	-

Figure D.1.3 Same as Figure D.1.2 but over the NDACC station of Scoresbysund (Eastern Greenland), measured by GOME-2C (GDP 4.9) and by the SAOZ UVVIS spectrometer (LATMOS fast-delivery processing) operated by CNRS/DMI.

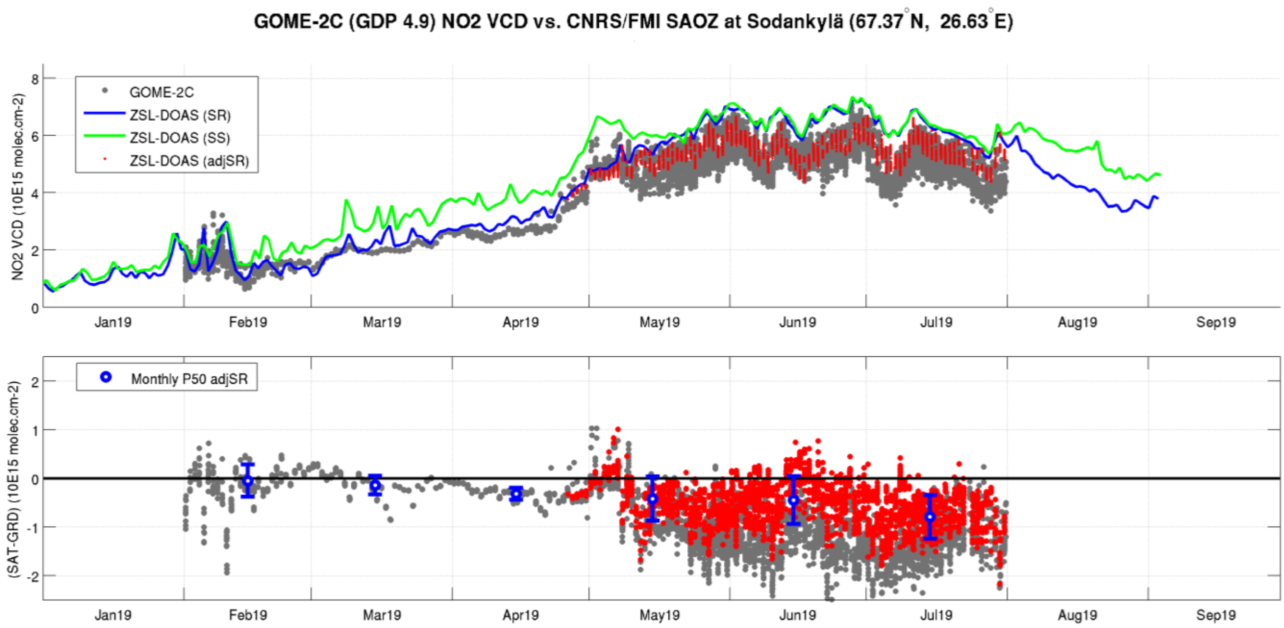

GOME2 NRT_OFL GDP 4.9 NO2 vertical column 8101 pixels in 181 days (01/02/2019 - 31/07/2019)			Sodankylä (67.37°N, 26.63°E) CNRS/FMI SAOZ (NC), source: LATMOS_RT 606 meas. in 304 days (01/11/2018 - 03/09/2019)				Method: zovp pixels (all CF) vs. Twilights Global agreement: -0.4 ± 0.5 (10^{15}mol.cm^{-2}) Linear drift: NaN*t (10^{15}mol.cm^{-2}/year), ϕ = NaN				
	January	February	March	April	May	June	July	August	September	October	November	December
2019	-	-0.0 ± 0.3	-0.1 ± 0.2	-0.3 ± 0.1	-0.4 ± 0.5	-0.4 ± 0.5	-0.8 ± 0.4	-	-	-	-	-

Figure D.1.4 Same as Figure D.1.2 but over the NDACC station of Sodankylä (Finland), measured by GOME-2C (GDP 4.9) and by the SAOZ UVVIS spectrometer (LATMOS RT processing) operated by CNRS/FMI-ARC.

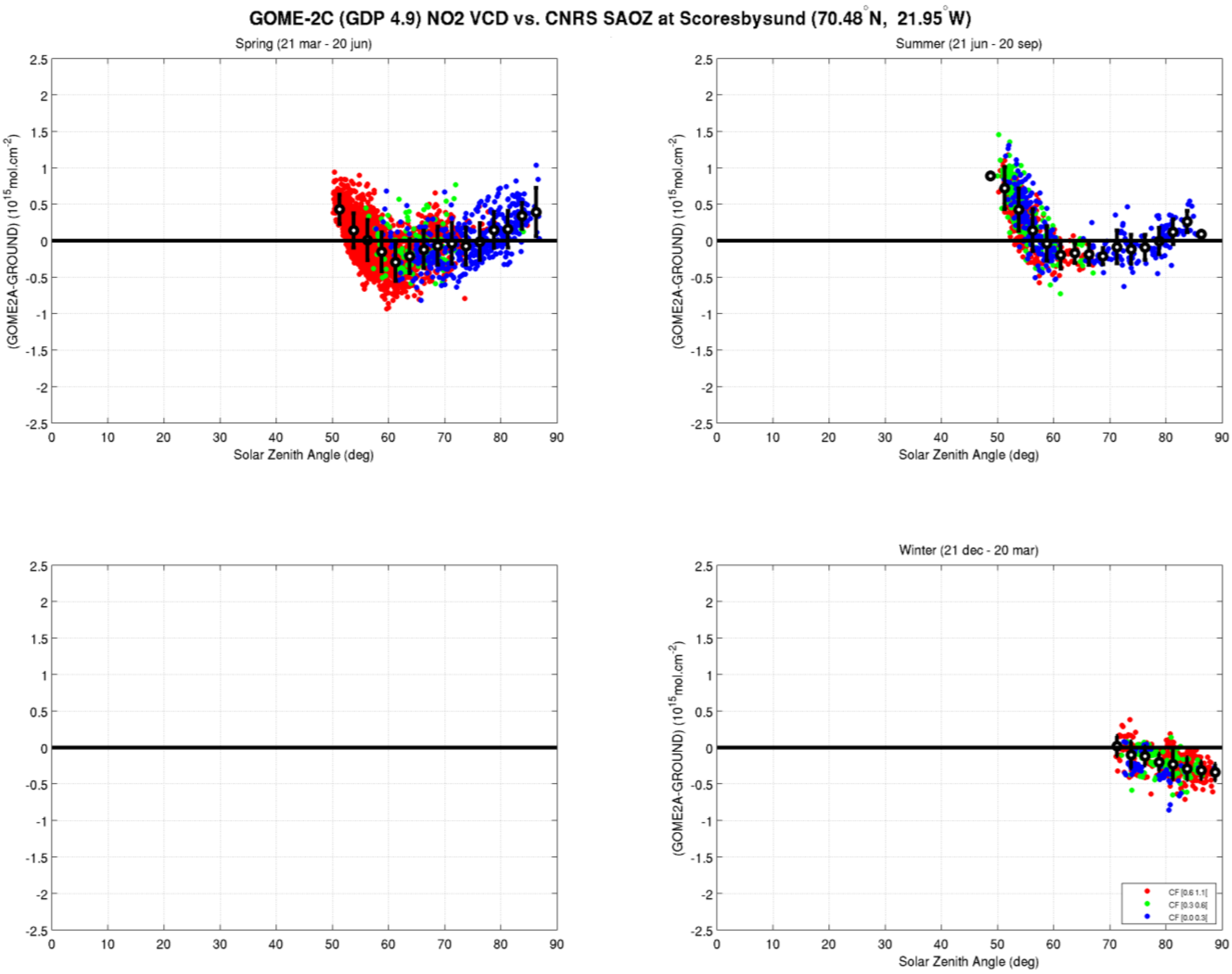

Figure D.1.5 Same as Figure D.1.2 at Scoresbysund (Greenland), but now the difference between GOME-2C (GDP 4.9) and the SAOZ UVVIS data is plotted as a function of the GOME-2C solar zenith angle and by season.

D.1.1.2 Stratospheric NO_2 column at Northern middle latitudes

Figures D.1.6 to D.1.8 present comparisons at three middle latitude stations in France: Paris, Guyancourt and O.H.P.. While Paris is permanently polluted and Guyancourt is located in the immediate vicinity of Paris, O.H.P. is considered as a background station, only episodically affected by tropospheric pollution. The median agreement between the various data sets is remarkable, of the order of a few 10^{14} molec.cm^{-2}. Seasonal changes in stratospheric NO_2 are captured similarly by GOME-2C and the SAOZ instruments. On the other hand, GOME-2C reports much smoother day-to-day changes of the stratospheric column than the three SAOZ instruments. This latter finding is in contrast with the much better agreement in day-to-day changes reported at Arctic latitudes in the previous subsection.

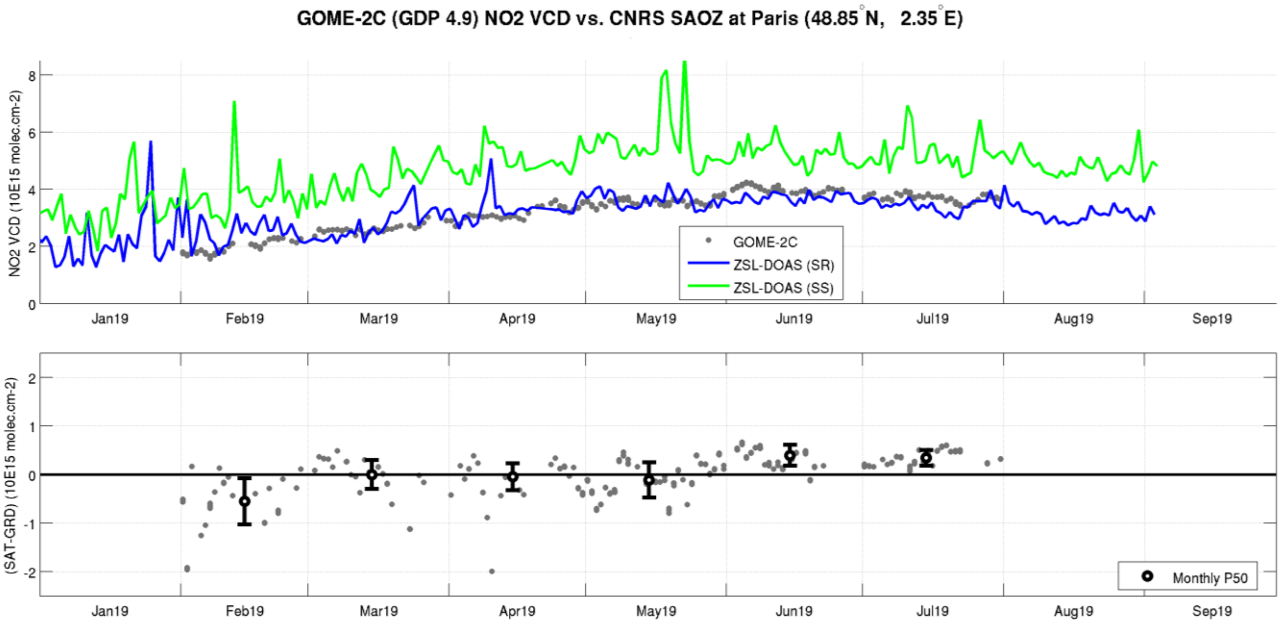

GOME2 NRT_OFL GDP 4.9 NO2 vertical column 640 pixels in 159 days (01/02/2019 - 31/07/2019)	Paris (48.85°N, 2.35°E) CNRS SAOZ (NC), source: LATMOS_RT 591 meas. in 303 days (01/11/2018 - 03/09/2019)	Method: zovp pixels (CF≥25%) vs. Twilights Global agreement: 0.1 ± 0.4 (10^{15}mol.cm^{-2}) Linear drift: NaN*t (10^{15}mol.cm^{-2}/year) , ϕ = NaN

	January	February	March	April	May	June	July	August	September	October	November	December
2019	-	-0.6 ± 0.5	-0.0 ± 0.3	-0.0 ± 0.3	-0.1 ± 0.4	0.4 ± 0.2	0.3 ± 0.2	-	-	-	-	-

Figure D.1.6 Same as Figure D.1.2 but over the station of Paris (France), measured by GOME-2C (GDP 4.9) and by the SAOZ UVVIS spectrometer (LATMOS RT processing) operated by CNRS/LATMOS.

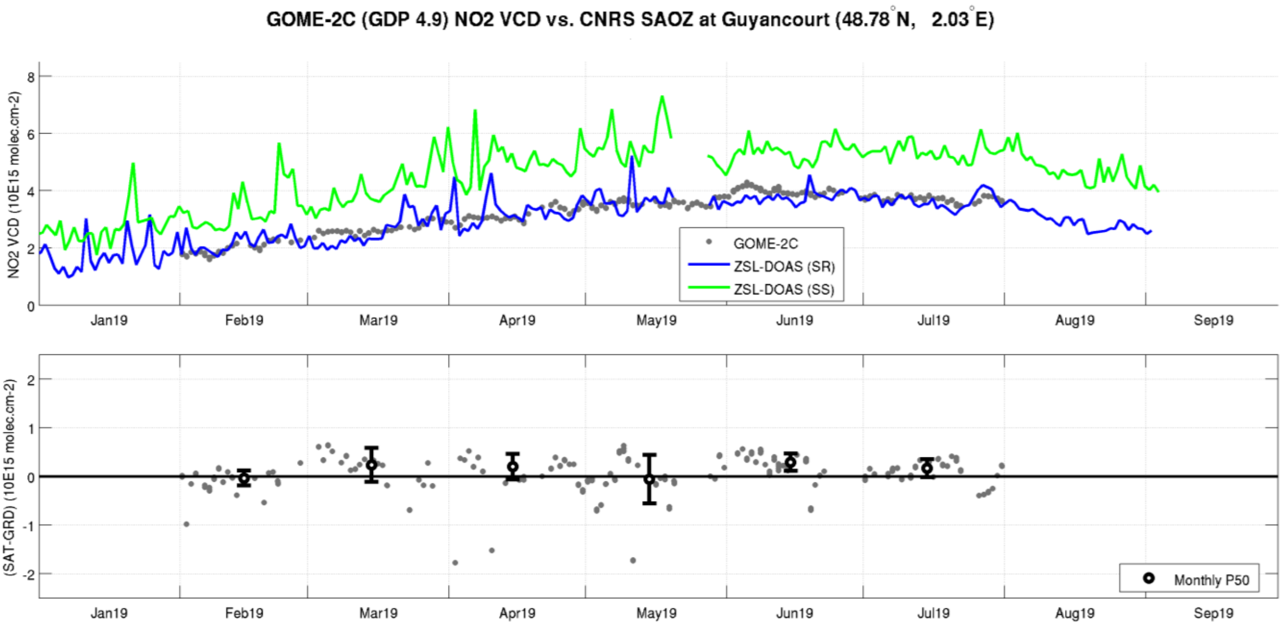

GOME2 NRT_OFL GDP 4.9 NO2 vertical column 621 pixels in 160 days (01/02/2019 - 31/07/2019)	Guyancourt (48.78°N, 2.03°E) CNRS SAOZ (NC), source: LATMOS_RT 582 meas. in 297 days (01/11/2018 - 03/09/2019)	Method: zovp pixels (CF≥25%) vs. Twilights Global agreement: 0.1 ± 0.3 (10^{15}mol.cm^{-2}) Linear drift: NaN*t (10^{15}mol.cm^{-2}/year) , ϕ = NaN

	January	February	March	April	May	June	July	August	September	October	November	December
2019	-	-0.0 ± 0.2	0.2 ± 0.3	0.2 ± 0.3	-0.1 ± 0.5	0.3 ± 0.2	0.2 ± 0.2	-	-	-	-	-

Figure D.1.7 Same as Figure D.1.2 but over the station of Guyancourt (France), measured by GOME-2C (GDP 4.9) and by the SAOZ UVVIS spectrometer (LATMOS RT processing) operated by CNRS/LATMOS.

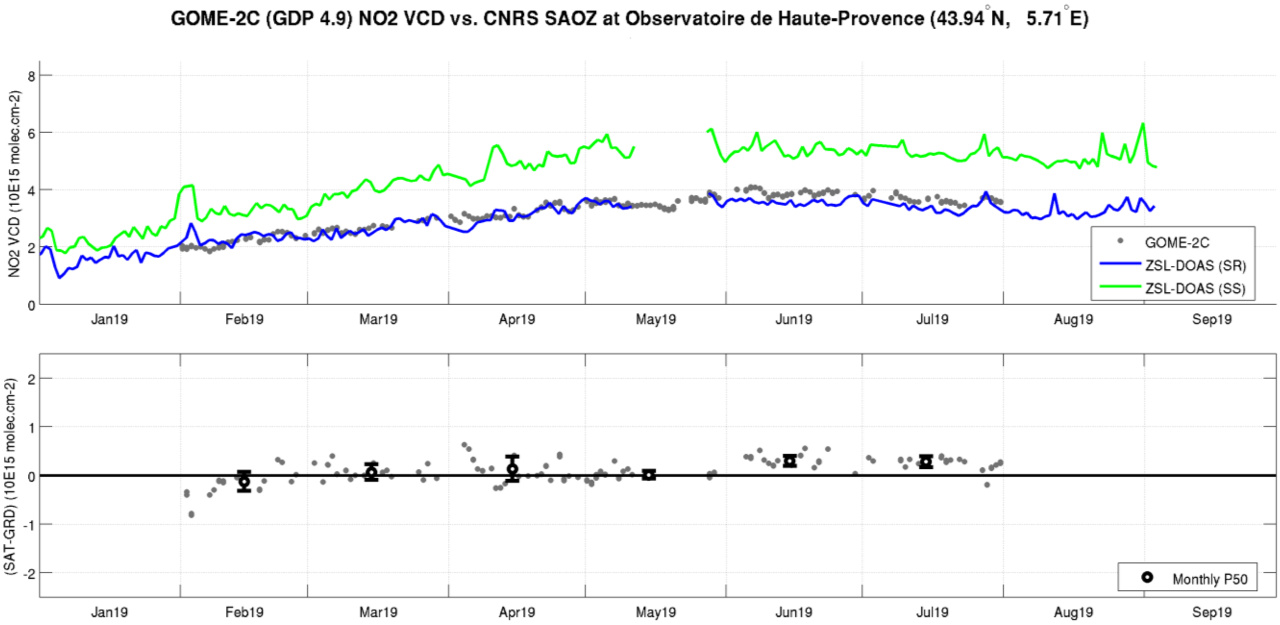

GOME2 NRT_OFL GDP 4.9 NO2 vertical column
421 pixels in 147 days (01/02/2019 - 31/07/2019)

Observatoire de Haute-Provence (43.94°N, 5.71°E)
CNRS SAOZ (CP200_NMOS1024), source: LATMOS_RT
534 meas. in 278 days (01/11/2018 - 03/09/2019)

Method: zovp pixels (CF≥25%) vs. Twilights
Global agreement: 0.1 ± 0.2 (10^{15}mol.cm^{-2})
Linear drift: NaN*t (10^{15}mol.cm^{-2}/year) , ϕ = NaN

	January	February	March	April	May	June	July	August	September	October	November	December
2019	-	-0.1 ± 0.2	0.1 ± 0.2	0.1 ± 0.3	0.0 ± 0.1	0.3 ± 0.1	0.3 ± 0.1	-	-	-	-	-

Figure D.1.8 Same as Figure D.1.2 but over the NDACC station of Observatoire de Haute Provence (O.H.P., Southern France), measured by GOME-2C (GDP 4.9) and by the SAOZ UVVIS spectrometer (LATMOS RT processing) operated by CNRS/LATMOS.

D.1.1.3 Stratospheric NO_2 column in the Southern tropics

Figures D.1.9 to D.1.10 present comparisons at two Southern tropical stations. At Saint Denis (Reunion Island, Figure D.1.9) the monthly median agreement between GOME-2C and the NDACC DOAS UVVIS NO_2 column data is within a few 10^{14} molec.cm^{-2}. At the Brazilian station of Bauru (Figure D.1.10) a systematic low bias of $7\cdot10^{14}$ molec.cm^{-2} appear between the satellite and ground-based data, probably due to the persistent pollution seen in this area by GOME-2C but less by the SAOZ. As reported in Northern middle latitudes, day-to-day changes of the stratospheric NO_2 column measured from the ground are smoothed by GOME-2C.

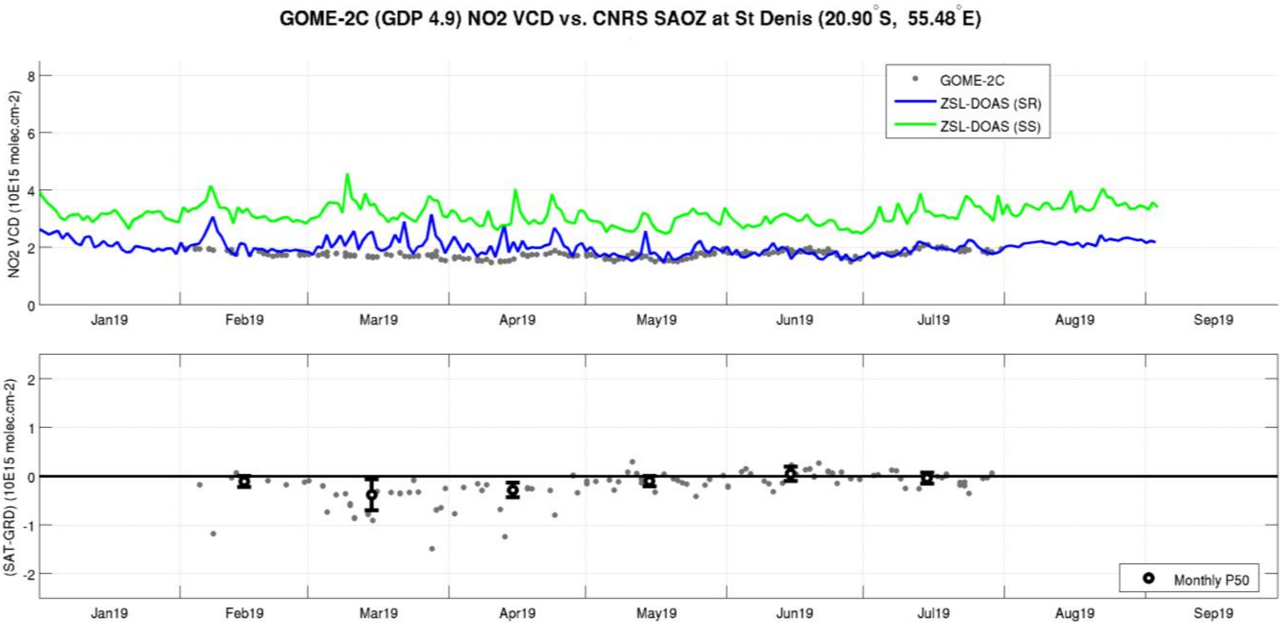

GOME2 NRT_OFL GDP 4.9 NO2 vertical column 241 pixels in 143 days (02/02/2019 - 31/07/2019)				St Denis (20.90°S, 55.48°E) CNRS SAOZ (CP200_NMOS1024), source: LATMOS_RT 591 meas. in 304 days (01/11/2018 - 03/09/2019)				Method: zovp pixels (all CF) vs. Twilights Global agreement: -0.2 ± 0.2 (10^{15}molec.cm^{-2}) Linear drift: NaN*t (10^{15}molec.cm^{-2}/year), ϕ = NaN				
	January	February	March	April	May	June	July	August	September	October	November	December
2019	-	-0.1 ± 0.1	-0.4 ± 0.3	-0.3 ± 0.2	-0.1 ± 0.1	0.0 ± 0.1	-0.0 ± 0.1	-	-	-	-	-

Figure D.1.9 Same as Figure D.1.2 but over the NDACC station of Saint Denis (Reunion Island), measured by GOME-2C (GDP 4.9) and by the SAOZ UVVIS spectrometer (LATMOS RT processing) operated by CNRS/LACy.

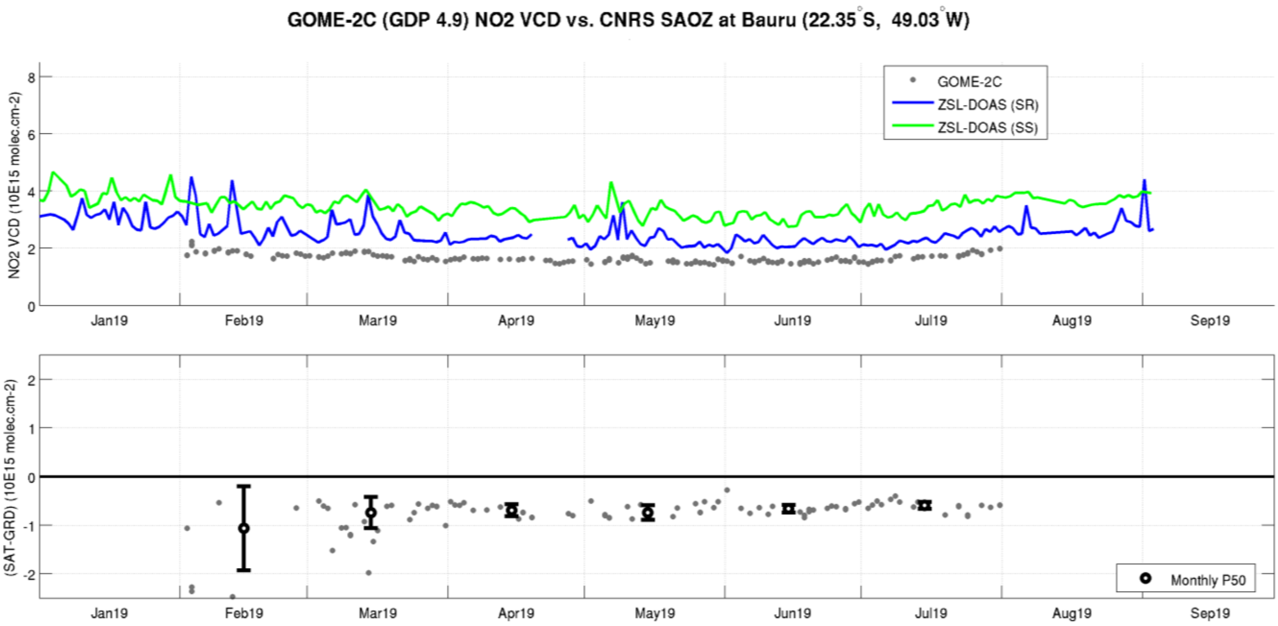

GOME2 NRT_OFL GDP 4.9 NO2 vertical column 227 pixels in 134 days (02/02/2019 - 31/07/2019)				Bauru (22.35°S, 49.03°W) CNRS SAOZ (CP200_NMOS1024), source: LATMOS_RT 539 meas. in 288 days (01/11/2018 - 03/09/2019)				Method: zovp pixels (all CF) vs. Twilights Global agreement: -0.7 ± 0.2 (10^{15}molec.cm^{-2}) Linear drift: NaN*t (10^{15}molec.cm^{-2}/year), ϕ = NaN				
	January	February	March	April	May	June	July	August	September	October	November	December
2019	-	-1.1 ± 0.9	-0.7 ± 0.3	-0.7 ± 0.1	-0.7 ± 0.1	-0.7 ± 0.1	-0.6 ± 0.1	-	-	-	-	-

Figure D.1.10 Same as Figure D.1.2 but over the NDACC station of Bauru (Brazil), measured by GOME-2C (GDP 4.9) and by the SAOZ UVVIS spectrometer (LATMOS RT processing) operated by CNRS/UNESP.

D.1.1.4 Stratospheric NO_2 column in the Southern middle latitudes

Figures D.1.11 to D.1.13 present comparisons at three NDACC stations distributed around the Southern middle latitudes (between 45° and 52°S): Lauder in New Zealand, Kerguelen in the Indian Ocean, and Rio Gallegos in Argentina. Those stations are, if never, at least rarely affected by tropospheric pollution. GOME-2C and NDACC ZLS-DOAS instruments – here of two different types: SAOZ and NIWA system – capture similarly the seasonal cycle of stratospheric NO_2, as well as monthly in stratospheric NO_2. In summer day-to-day changes observed from the ground are smoothed by GOME-2C, while enhanced dispersion appears in GOME-2C data in fall. Quantitatively, results at Lauder in New Zealand conclude to a large negative bias ranging from $10 \cdot 10^{14}$ molec.cm^{-2} in summer to $5 \cdot 10^{14}$ molec.cm^{-2} in winter, likely due to the provisional character of the ground-based data processing.

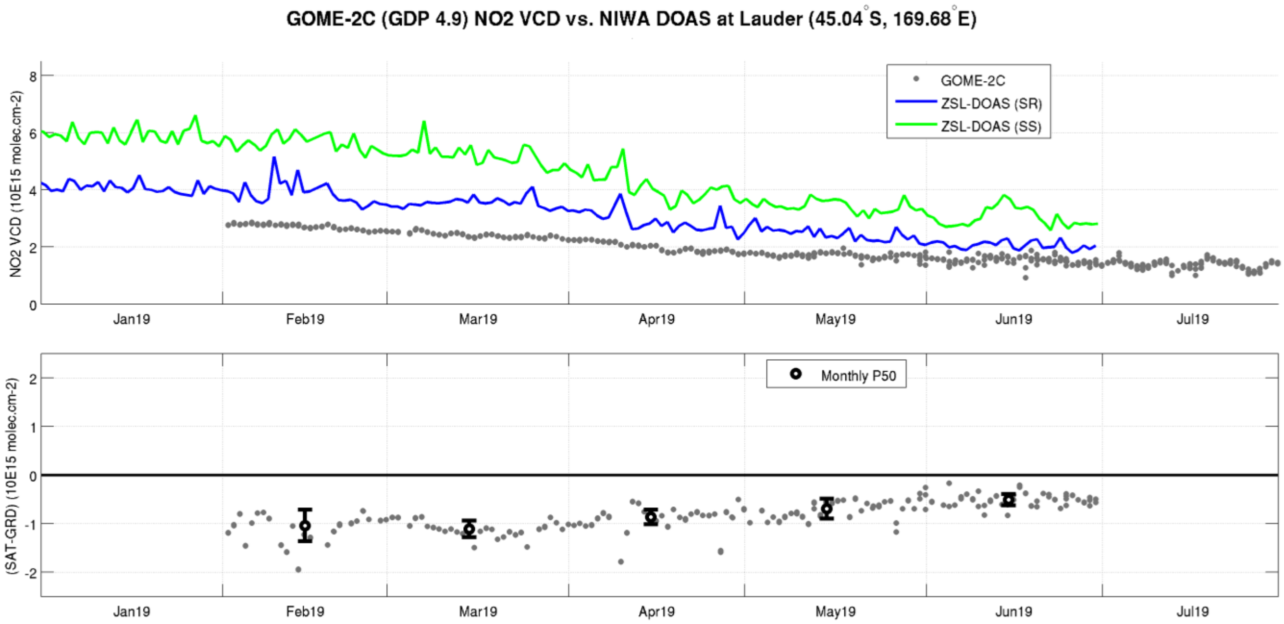

GOME2 NRT_OFL GDP 4.9 NO2 vertical column
767 pixels in 180 days (01/02/2019 - 31/07/2019)

Lauder (45.04°S,169.68°E)
NIWA DOAS (NC), source: NDACC
467 meas. in 236 days (01/11/2018 - 30/06/2019)

Method: zovp pixels (all CF) vs. Twilights
Global agreement: -0.9 ± 0.3 (10^{15}mol.cm^{-2})
Linear drift: NaN*t (10^{15}mol.cm^{-2}/year) , ϕ = NaN

	January	February	March	April	May	June	July	August	September	October	November	December
2019	-	-1.0 ± 0.3	-1.1 ± 0.2	-0.9 ± 0.1	-0.7 ± 0.2	-0.5 ± 0.1	-	-	-	-	-	-

Figure D.1.11 Same as Figure D.1.2 but over the NDACC station of Lauder (New Zealand), measured by GOME-2C (GDP 4.9) and by the ZLS-DOAS UVVIS spectrometer operated by NIWA.

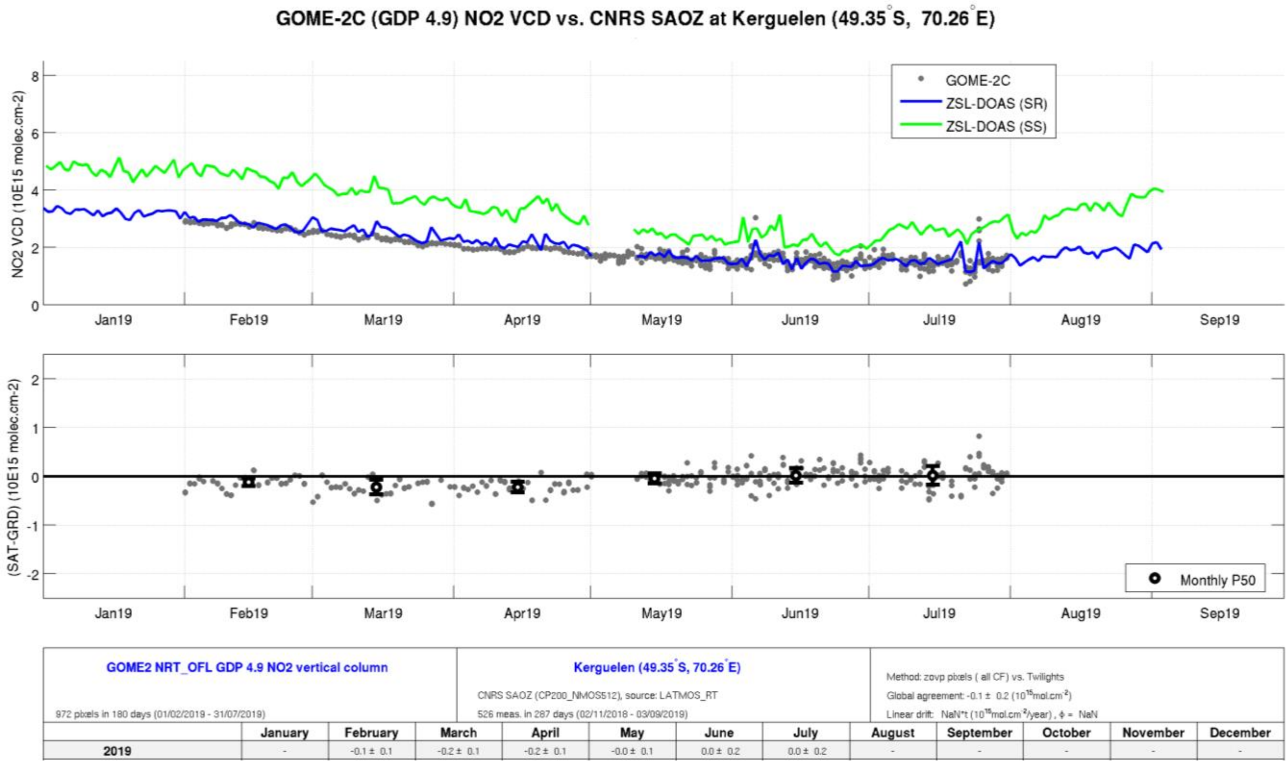

Figure D.1.12 Same as Figure D.1.2 but over the NDACC station of Kerguelen Island (Indian Ocean), measured by GOME-2C (GDP 4.9) and by the SAOZ UVVIS spectrometer (LATMOS RT processing) operated by CNRS/LATMOS.

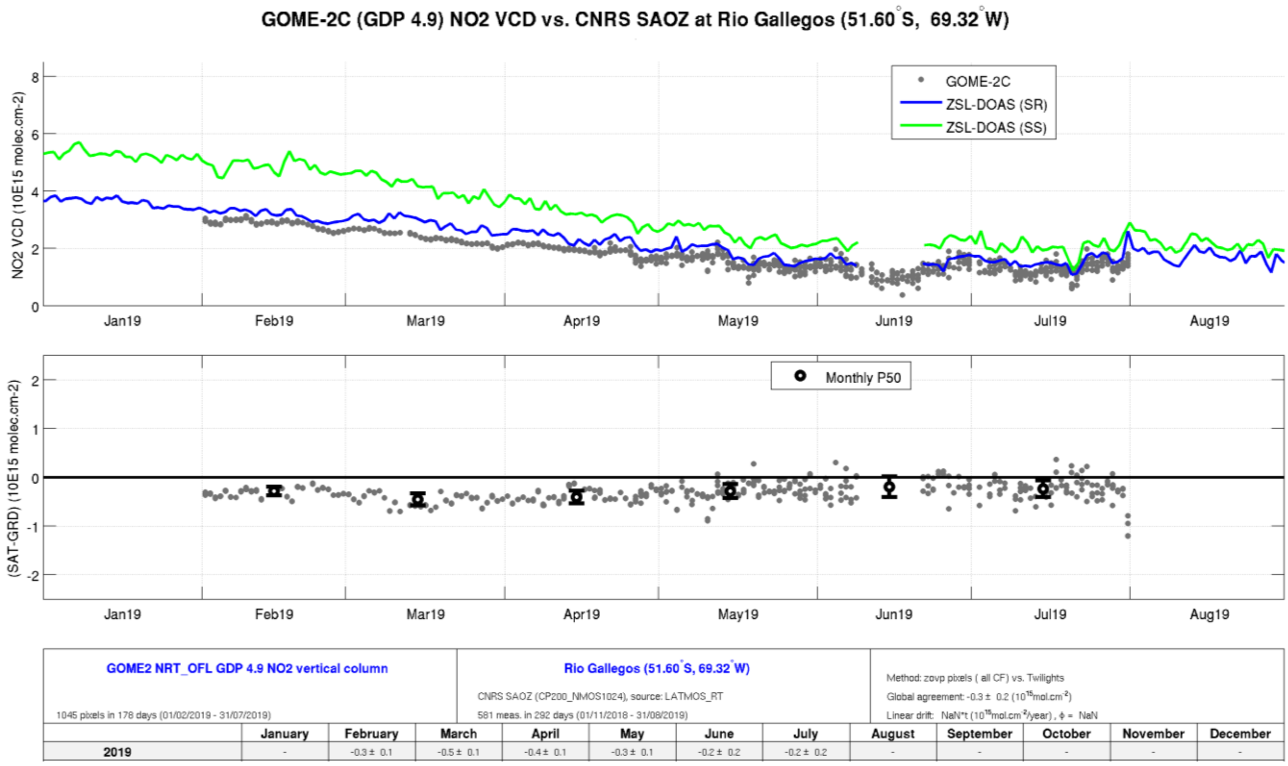

Figure D.1.13 Same as Figure D.1.2 but over the NDACC station of Rio Gallegos (Argentina), measured by GOME-2C (GDP 4.9) and by the SAOZ UVVIS spectrometer (LATMOS RT processing) operated by CNRS/LATMOS.

D.1.1.5 Stratospheric NO_2 column in Antarctica

Figures D.1.14 and D.1.15 report comparisons at the NDACC Antarctic stations of Dumont d'Urville and Dome Concorde. Those stations in pristine environment are free of any tropospheric pollution. During polar day, GOME-2C data are distributed in two tracks: one orbit of GOME-2 data acquired in the mid-morning, under moderate SZA, and a second orbit of GOME-2 data closer to midnight sun conditions, acquired at larger SZA, which explains the apparent enhanced dispersion of GOME-2C data in Antarctic summer. This dispersion disappears after appropriate data filtering on SZA. To avoid interferences of diurnal cycle effects with the comparison results, only GOME-2 data acquired at SZA larger than 75° have been selected here to draw statistical conclusions. At the end of summer the midnight sun track disappears and the solar local time difference between mid-morning GOME-2 data and twilight ground-based data is too large to avoid unbiased comparisons. In fall this local time difference vanishes progressively.

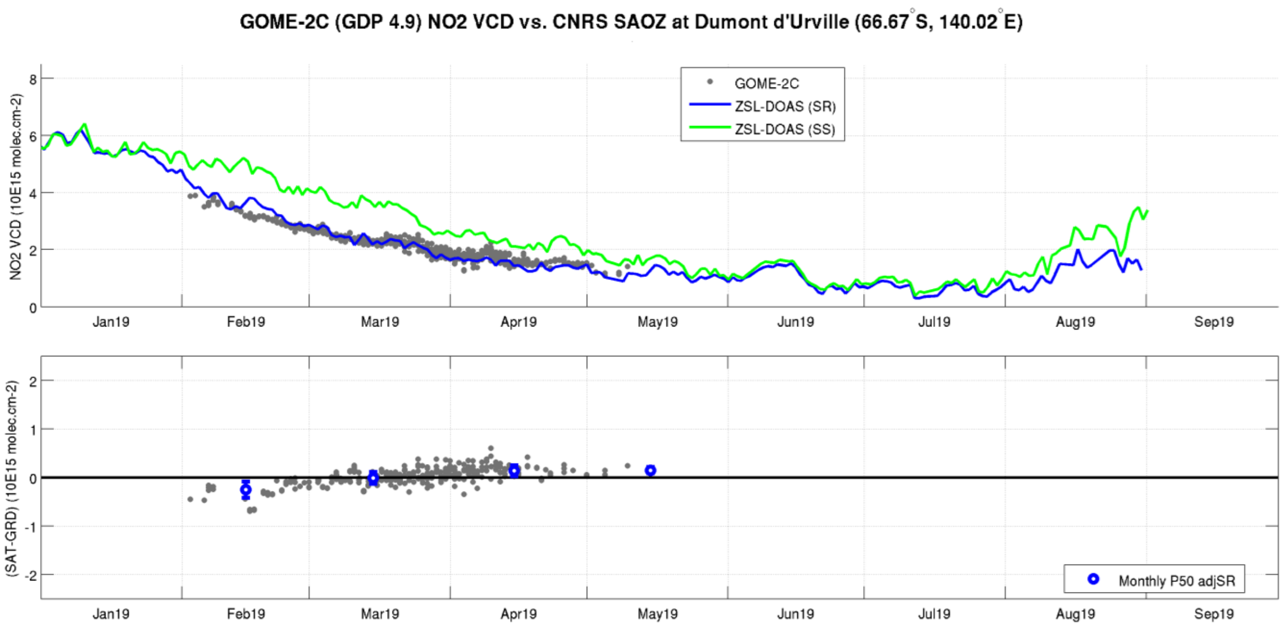

GOME2 NRT_OFL GDP 4.9 NO2 vertical column 849 pixels in 89 days (02/02/2019 - 09/05/2019)				Dumont d'Urville (66.67°S,140.02°E) CNRS SAOZ (CP200_NMOS1024), source: LATMOS_RT 573 meas. in 297 days (01/11/2018 - 01/09/2019)				Method: zovp pixels (all CF) vs. Twilights Global agreement: 0.0 ± 0.2 (10^{15}mol.cm^{-2}) Linear drift: NaN*t (10^{15}mol.cm^{-2}/year) , ϕ = NaN				
	January	February	March	April	May	June	July	August	September	October	November	December
2019	-	-0.3 ± 0.2	-0.0 ± 0.1	0.1 ± 0.1	0.2 ± 0.1	-	-	-	-	-	-	-

Figure D.1.14 Same as Figure D.1.2 but over the NDACC station of Dumont d'Urville (Antarctica), measured by GOME-2C (GDP 4.9) and by the SAOZ UVVIS spectrometer (LATMOS RT reprocessing) operated by CNRS/LATMOS.

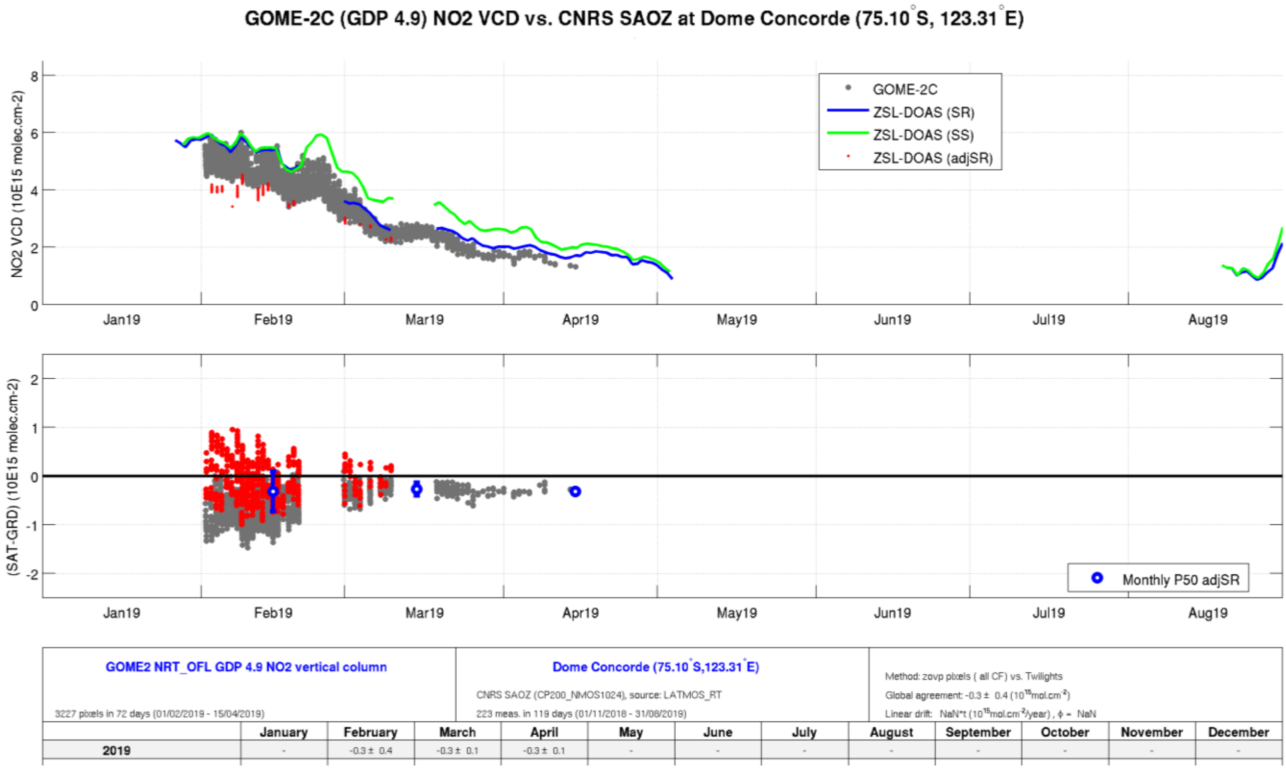

Figure D.1.15 Same as Figure D.1.2 but over the NDACC station of Dome Concorde (Antarctica), measured by GOME-2C (GDP 4.9) and by the SAOZ UVVIS spectrometer (LATMOS RT processing) operated by CNRS/LATMOS.

D.1.2 Stratospheric comparisons summary

In an attempt to summarize the GOME-2C initial validation results reported here above, and to compare them with similar validation studies of the operational GOME-2A and GOME-2B NO_2 data sets (based on the closest triple co-location events), Figure D.1.16 displays median difference values at all stations in the form of the classical pole-to-pole graph adopted in all AC SAF reports for GOME-2A and GOME-2B. Based on the data filtering and selection described in the previous subsections (application or not of cloud mask, selection on SZA at polar stations etc.) the comparison results yield sufficiently robust median difference estimates to be also summarized as in the following table, displaying the median bias between GOME-2 and ground-based zenith-sky column data:

Station name	Lat.	Long.	METOP-C GDP 4.9	METOP-A GDP 4.8	METOP-B GDP 4.8
Ny-Ålesund (NOR)	78.93	11.93	-0.90	-0.93	-0.98
Scoresbysund (GRL)	70.48	-21.95	-0.03	-0.05	-0.16
Sodankylä (FIN)	67.37	26.63	-0.44	-0.49	-0.62
Aberystwyth (GBR)	52.40	-4.10	-0.42	-0.55	-0.69
Paris (FRA)	48.85	2.35	0.12	-0.02	-0.08
Guyancourt (FRA)	48.78	2.03	0.15	0.01	-0.10
Observatoire de Haute-Provence (FRA)	43.94	5.71	0.10	0.07	-0.06
St Denis (REU)	-20.90	55.48	-0.15	-0.21	-0.18
Bauru (BRA)	-22.35	-49.03	-0.65	-0.72	-0.72
Lauder (NZL)	-45.04	169.68	-0.86	-0.96	-0.92
Kerguelen (FRA)	-49.35	70.26	-0.10	-0.25	-0.20
Rio Gallegos (ARG)	-51.60	-69.32	-0.32	-0.50	-0.44
Dumont d'Urville (ATA)	-66.67	140.02	0.00	-0.13	-0.11
Dome Concorde (ATA)	-75.10	123.31	-0.30	-0.55	-0.37

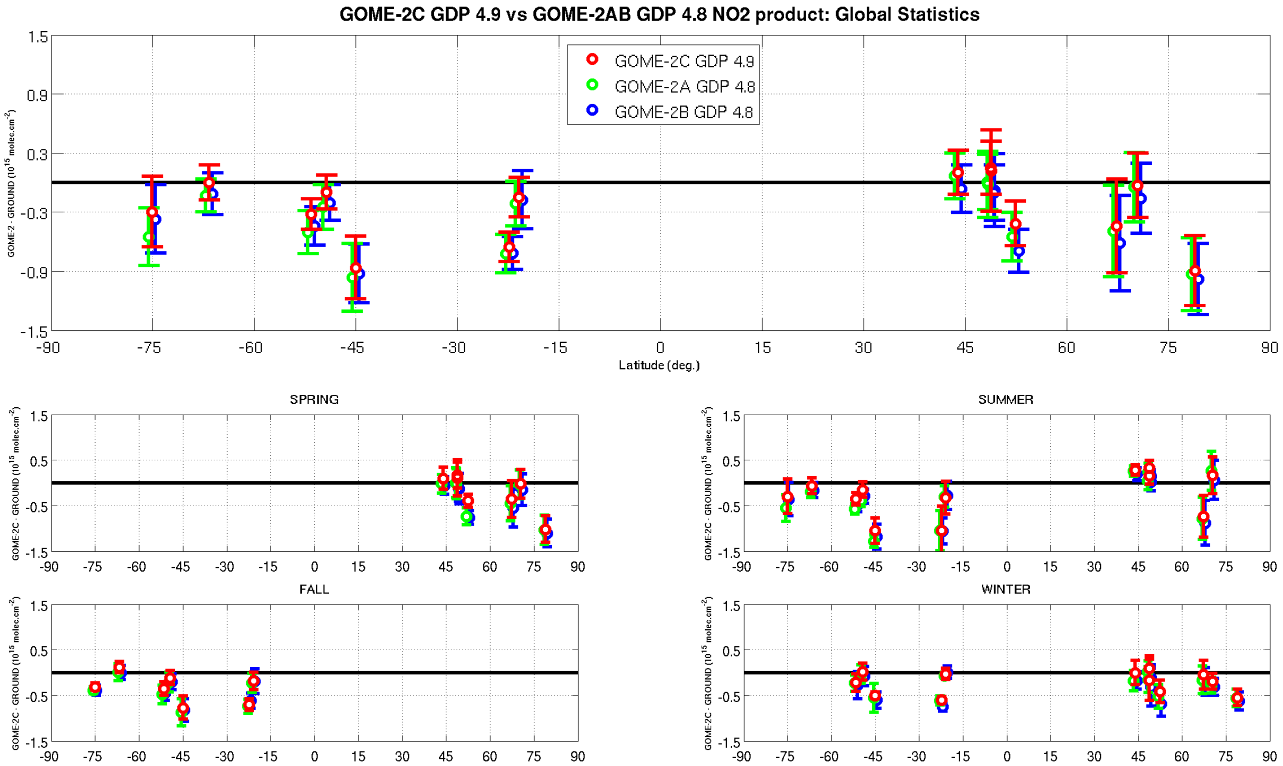

Figure D.1.16 Pole-to-pole overview of the median difference at each station between NO_2 column data reported by GOME-2C (GDP4.9), GOME-2A/B (GDP 4.8) and by 14 NDACC ground-based ZLS-DOAS spectrometers. Uncertainty estimates have been omitted for clarity.

From this summary plot D.1.16 and from details reported in previous subsections it can be concluded that:

- With respect to 14 NDACC ZLS-DOAS UV-visible spectrometers having provided provisional fast-delivery data sets, the MetOp-C GOME-2 NO_2 column data set available at the time of this report and processed with GDP 4.9, offers the same level of consistency as GOME-2A and GOME-2B GDP 4.8 do.
- Median bias: In most of the cases, GOME-2C reports NO_2 column values within $1\text{-}3 \cdot 10^{14}$ molec.cm^{-2} from the ground-based values, which is close to the combined uncertainty of ground-based NDACC measurements and of the comparison method.
- Dispersion: Under many conditions, day-to-day fluctuations of the stratospheric NO_2 column seem to be smoothed by GOME-2C, in comparison to the fluctuations reported by ground-based instruments.
- Variations of the stratospheric NO_2 column at seasonal scale are captured consistently by all measurement systems.
- In ideal comparison conditions the agreement between satellite data and network data does not depend significantly on GOME-2 solar zenith angle and fractional cloud cover. Apparent dependences on the SZA in more difficult conditions might be associated with the provisional character of the ground-based data processing and on remaining diurnal cycle effects.
- Further investigation based on reprocessed ground-based data with state-of-the-art algorithms needs to be done to confirm current provisional conclusions on GOME-2C data quality and to elucidate apparent dependences.

D.2. Tropospheric Vertical Column

D.2.1 Comparison against ground-based MAX-DOAS columns data

The different MAXDOAS instruments used in this study are presented in Figure D.2.1. A good coverage of the Northern Hemisphere is assured, with several stations in Europe, South America and Asia, but only one stations measured in the Southern Hemisphere: la_reunion_maido. A few of these stations report vertical profiles (Clémer et al 2010, Hendrick et al., 2014, Irie et al., 2008, Vlemmix et al., 2010; 2014, Wagner et al., 2011, Friedrich et al., 2019) but in this preliminary study we only focus on the tropospheric vertical columns.

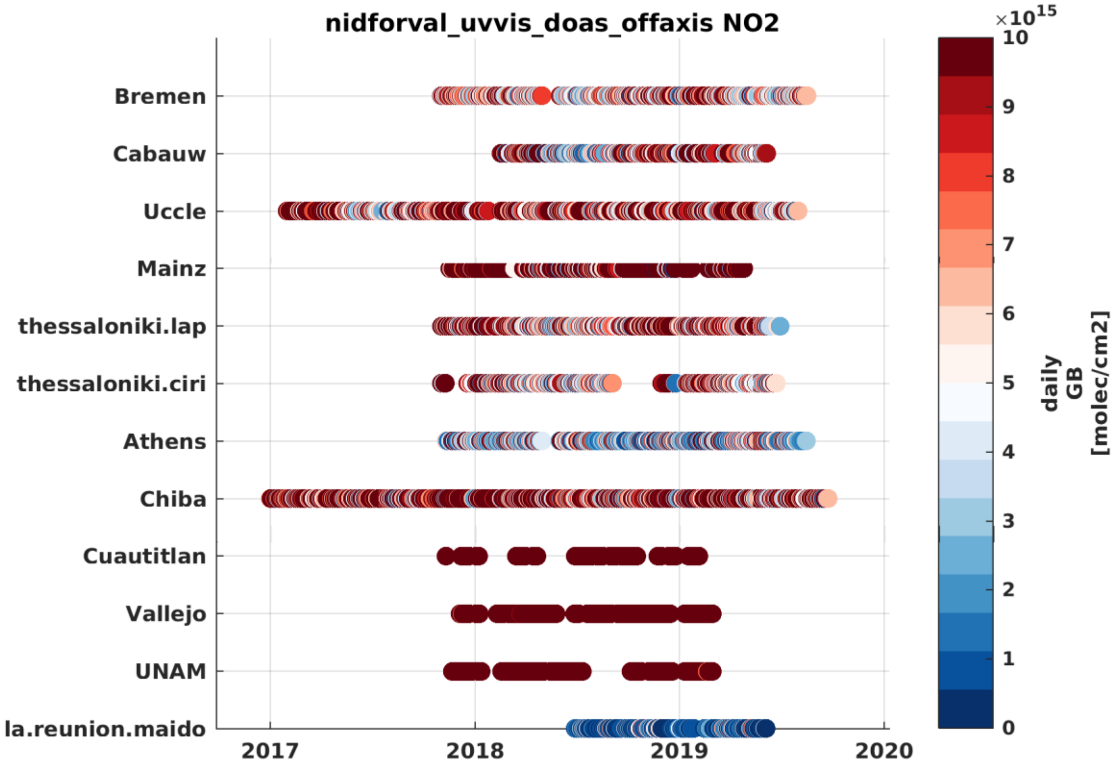

Figure D.2.1 List of MAXDOAS instruments used in this study and their temporal coverage. The time-series are color-coded with their respective tropospheric NO_2 VCD values.

GOME-2 data are extracted within 50 km of the different stations and only closest pixels with a valid tropospheric NO_2 flag for each day are kept for the comparison. The ground-based MAXDOAS data are interpolated at the satellite overpass time. Daily and monthly comparisons are performed, and an overview of the time-series of tropospheric NO_2 columns from GOME-2C and MAXDOAS for nine stations is presented in Figure D.2.2. Scatter plots of the daily and monthly points are presented in Figure D.2.3. As for comparisons performed in past GOME-2 validation exercises, GOME-2C tend to systematically display smaller columns than ground-based MAXDOAS measurements, especially in urban locations, likely due to the effect of strong local NO_2 emissions seen by ground-based instruments but smeared out at the coarse resolution of the GOME-2 observations 40x80 km^2 (NO_2 ACSAF VR 2017; Pinardi et al., in preparation). From the monthly mean values scatter plot, a global correlation coefficient of 0.83 is obtained, with a slope of about 0.49 (Figure D.2.3), strongly influenced by the large ground-based columns in Mexico (UNAM, Vallejo). Better results are obtained when only focusing in remote and suburban locations, with correlation of 0.92 and slope of 0.75 (figure D.2.4).

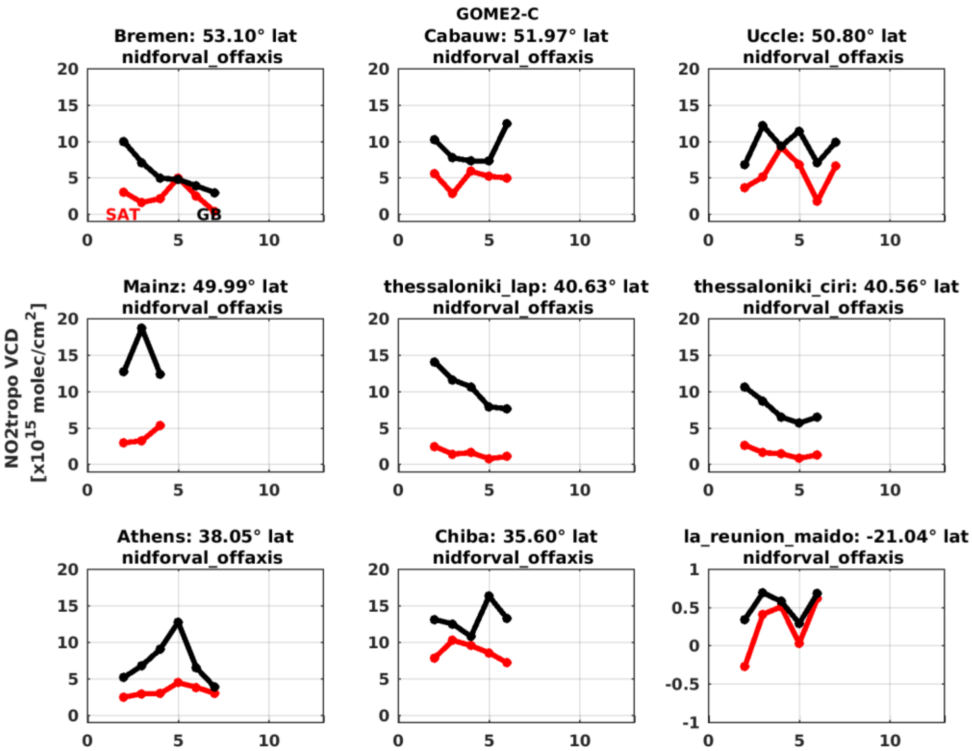

Figure D.2.2 Monthly mean tropospheric NO_2 column time series comparison GOME-2C GDP 4.9 (red) and the ground-based MAXDOAS data (black), between February and July 2019.

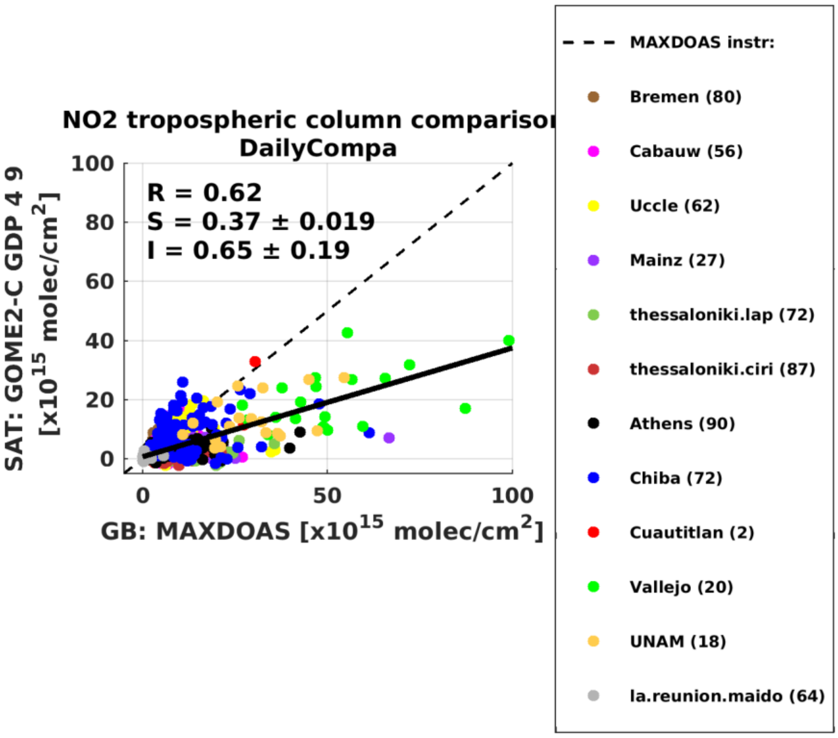

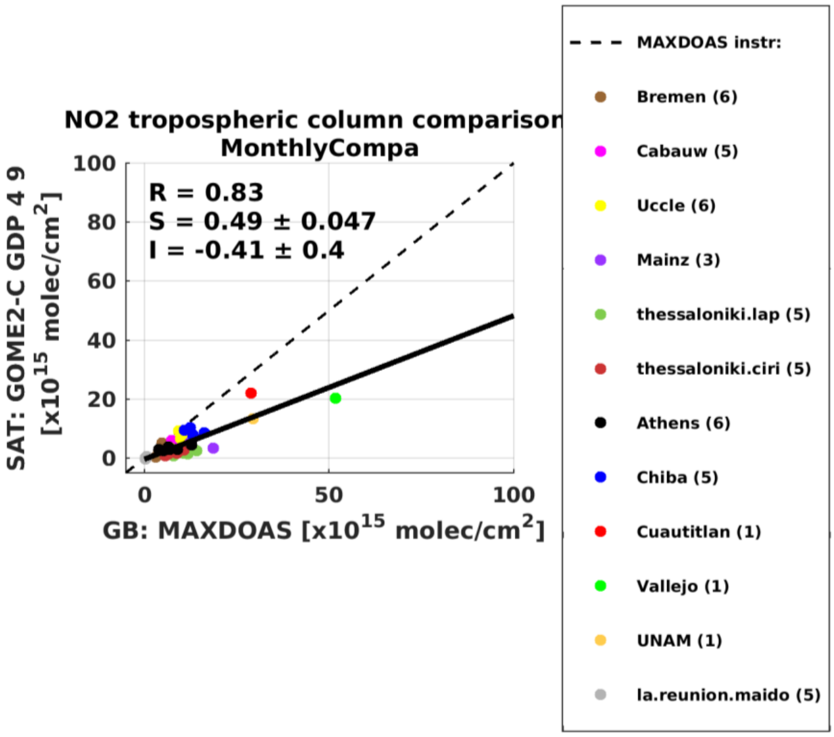

Figure D.2.3 Tropospheric NO_2 VCD scatter plot between GOME-2C GDP 4.9 satellite data and MAXDOAS ground-based data at the 12 stations included in the study. Daily (upper panel) and monthly (lower panel) are included.

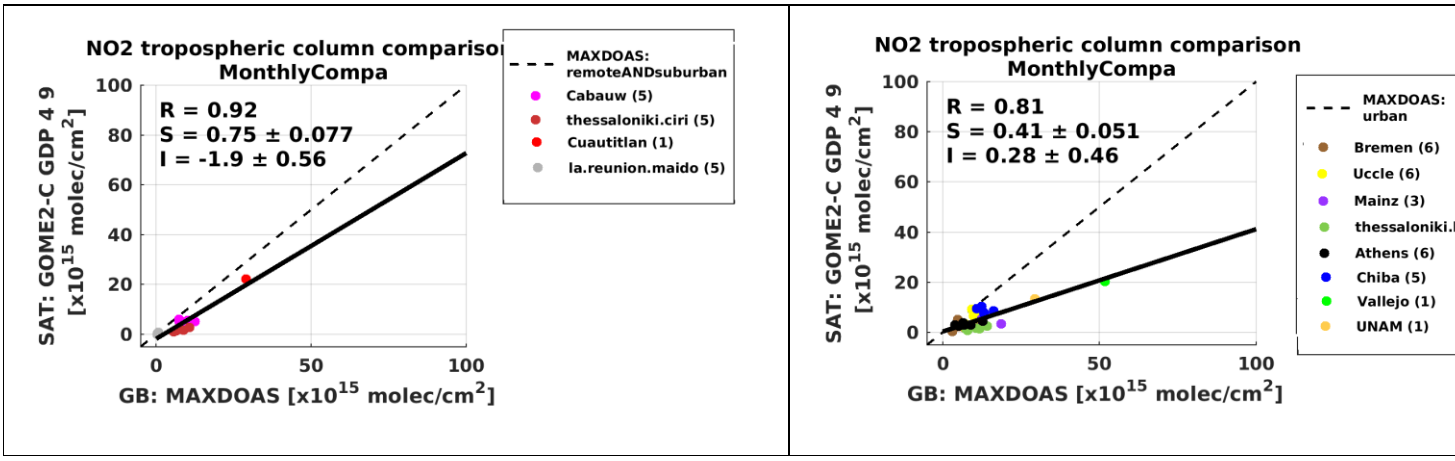

Figure D.2.4 Same as Figure D.2.3 but dividing into (a) suburban and remote, (b) urban sites.

Figure D.2.5 presents the equivalent results obtained for the GOME-2B data in the same period of time (February to July 2019). Results are similar, with correlation coefficient of 0.8, largely affected by the comparisons at the Mexican sites, and a general under-estimation, even larger for GOME-2B (smaller slope of 0.29).

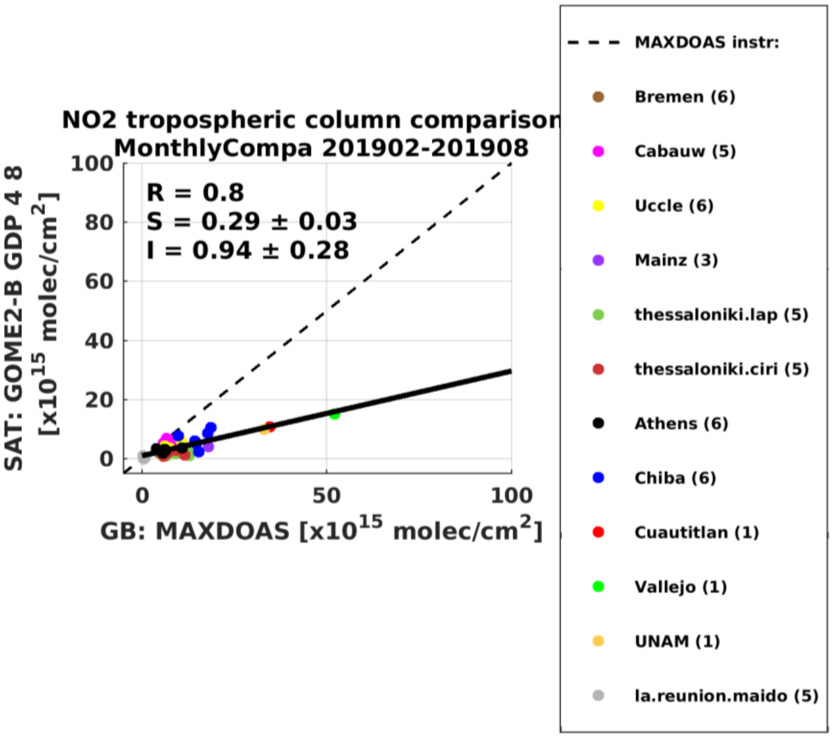

Figure D.2.5 Same as Figure D.2.3 but for GOME-2B measurements in GOME-2C time-period.

D.3. Total Vertical Column

The direct comparison of GOME-2 total NO_2 is focusing on comparisons with direct-sun instruments, as performed with scientific direct-sun mode DOAS instruments and Pandora direct-sun network in Pinardi et al. (2014) for GDP 4.7 and in Pinardi et al. (in preparation) for GDP 4.8.

D.3.1 Comparison against ground-based Direct-sun columns data

The different direct-sun instruments used in this study are illustrated in Figure D.3.1. These include seven Pandora systems from the PGN (https://www.pandonia-global-network.org), covering polluted areas (several instruments in Rome and New York city), and Izana and Mauna Loa remote cases.

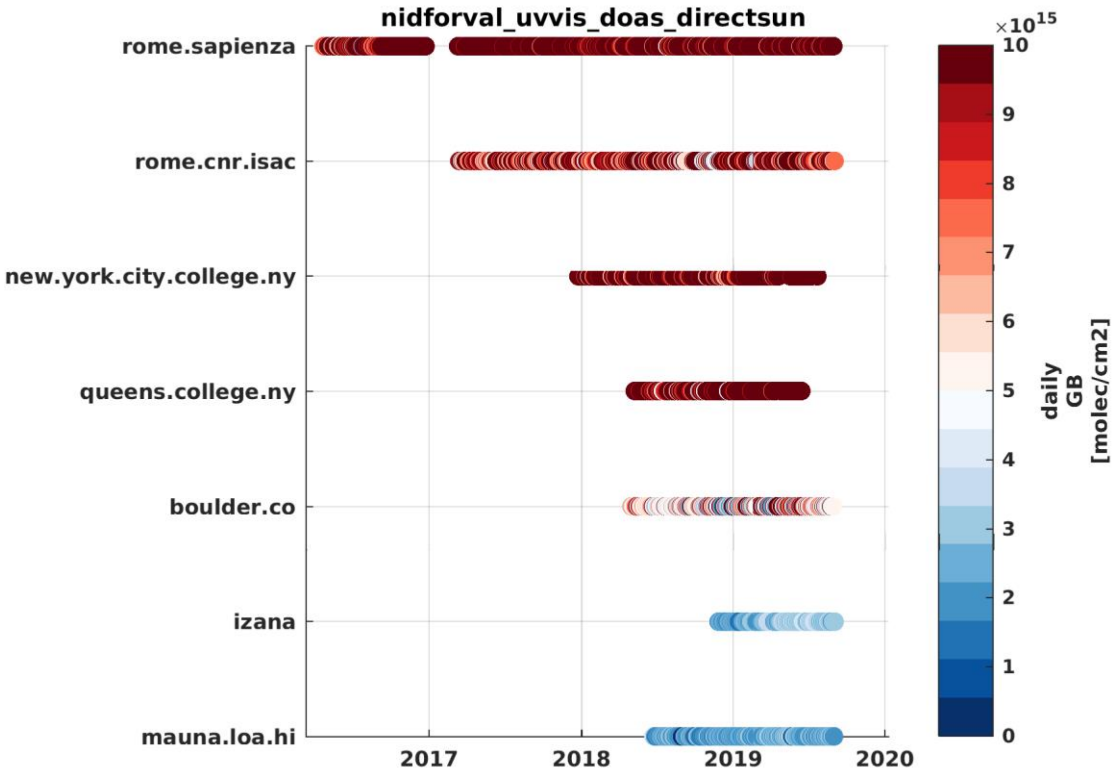

Figure D.3.1 List of direct-sun instruments used in this study and their temporal coverage. . The time-series are color-coded with their respective total NO_2 VCD values.

As for the tropospheric comparisons, the GOME-2 data are extracted within 50 km of the different stations and closest daily pixel with a valid tropospheric NO_2 flag are selected. The ground-based data are interpolated at the satellite overpass time for further comparison. Total columns (stratospheric plus tropospheric values from the satellites) are compared in Figure D.3.2 and D.3.3. As for the MAXDOAS comparisons, GOME-2 values are smaller than the ground-based measurements, but results are quite coherent between GOME-2C and GOME-2B. Good correlation coefficients is found (0.89 and 0.75) and the slope is smaller than 0.5.

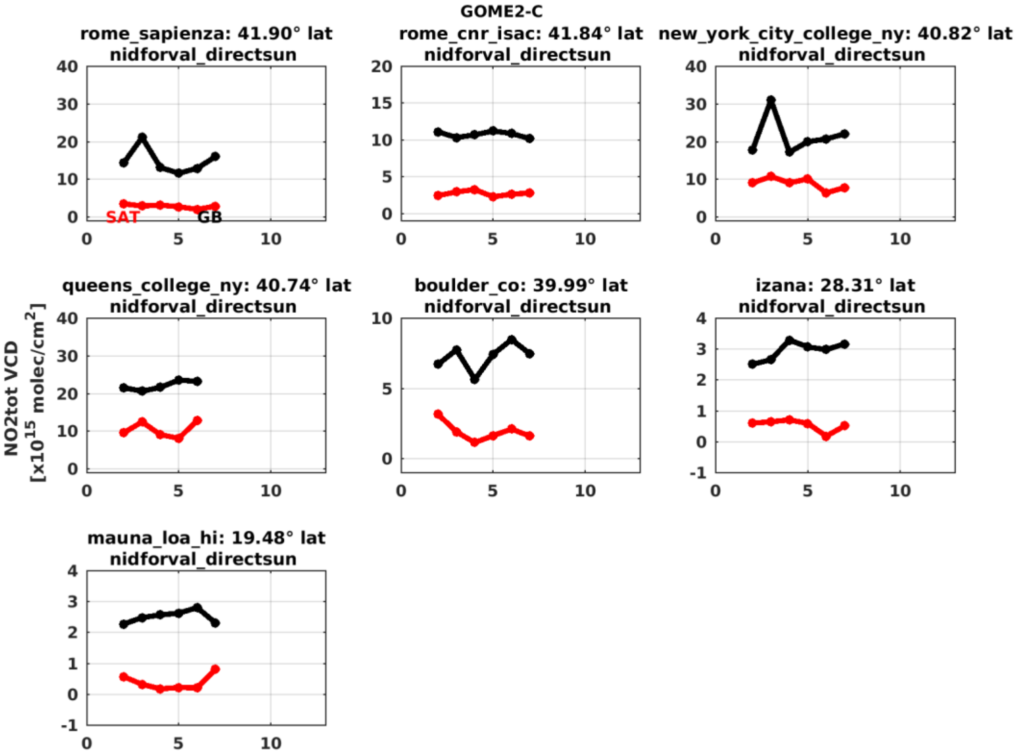

Figure D.3.2 NO_2 total column time series of GOME-2C GDP 4.8 (red) and the ground-based direct-sun data (black), between February and July 2019.

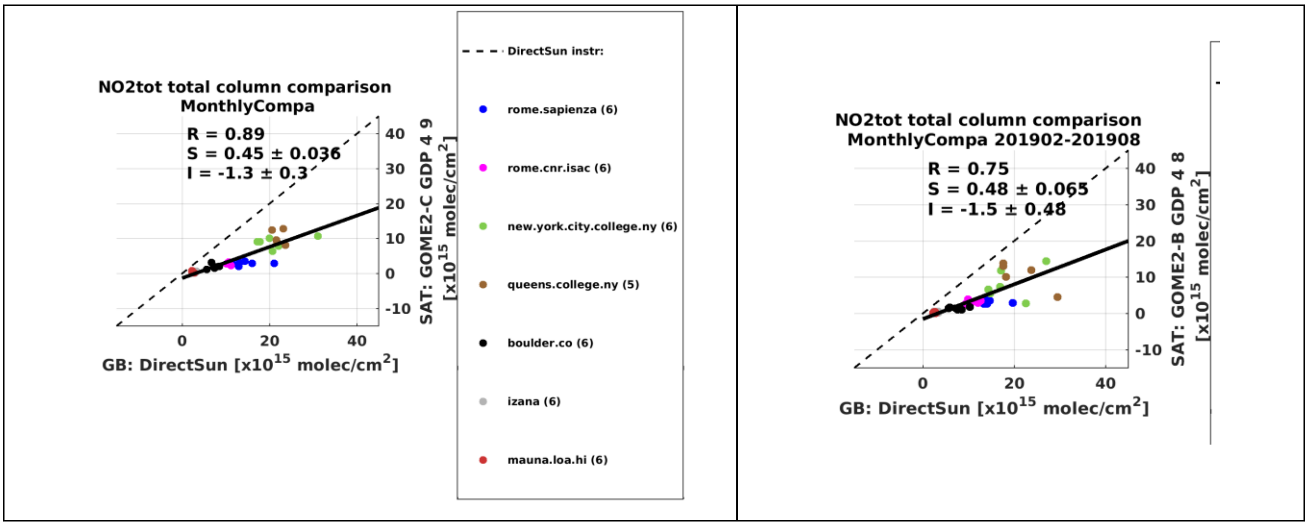

Figure D.3.3 Total NO_2 VCD scatter plot between GOME-2 satellite data and direct-sun ground-based data at the 7 stations included in the study. (left panel): GOME-2C results, (right panel): GOME-2B results on the same time-period.

E. CONCLUSION AND PERSPECTIVES

This document reports on the validation of AC SAF GOME-2 C NO_2 column data products retrieved at DLR with versions 4.9 of the GOME Data Processor (GDP).

The following main conclusions can be drawn:

- The GOME-2 C NO_2 slant columns generation from DOAS analysis had to be adapted in version GDP 4.9 to reduce the impact of resolution changes and L1 calibration issues. A fitting window covering 430.2–465nm has been applied to GOME-2C. This leads to geographically coherent slant columns, similar to GOME-2B results, but slightly larger above land and high latitude regions. The slant column scatter is about 10% larger in GOME-2B.
- GOME-2C seems to be less affected by the Southern Atlantic Anomaly (SAA) than previous instruments (better instrument shielding?). This should allow for better measurements in tropical South America.
- The systematic bias on the slant columns is transferred to the stratospheric vertical columns. The GOME-2C stratospheric columns are globally larger than GOME-2B, with a latitudinal structure with minimum differences around the equator and an increase at higher latitude (0.5~1e15 molec/cm^2).
- Validity of the tropospheric AMF calculation pixels selection has been found to lead to positive bias in the GOME-2B tropospheric columns between 30°S-0°S, leading to biases with GOME-2C. Based on the monthly averaged maps (gridded at 0.5°×0.5°) from February to July 2019, the difference in tropospheric vertical column density between GOME-2B and GOME-2C is ~32% (between 70°S and 70°N, and excluding the SAA regions) for pixels with VCD values exceeding 0.5×10^{15} molecules/cm^2. If only pixels with VCD larger than 2.5×10^{15} molecules/cm^2 are considered, the average difference between GOME-2B and GOME-2C is within 17%. It meets the optimal accuracy of requirement for tropospheric NO_2 (20%).
- The stratospheric NO_2 differences (negative bias over land and high latitudes mainly due to slant column changes) and tropospheric NO_2 differences (positive bias between 30^{o}S and 0^o in the average map related to difference in the data selection criteria) are combined and transferred to the total NO_2 columns. Based on the monthly February to July 2019 averaged data (gridded at 0.5°×0.5°), the difference in total NO_2 vertical column density between GOME-2B and GOME-2C is 2.5×10^{14} molecules/cm^2 (between 70°S and 70°N), which reach the optimal accuracy ($1\text{-}3\times10^{14}$) of the requirement.
- The GOME-2C temporal evolution of the different component of the retrieval is in good agreement with the GOME-2B in average over a few sites with different pollution conditions. Slightly larger differences appear for GOME-2A, probably due to degradation issues and smaller pixels.
- With respect to 14 NDACC ZLS-DOAS UV-visible spectrometers, the MetOp-C GOME-2 GDP 4.9 NO_2 column data, offers the same level of consistency as GOME-2A and GOME-2B GDP 4.8 do. In term of median bias, GOME-2C reports NO_2 column values in most of the cases within $1\text{-}3\cdot10^{14}$ molec.cm-2 from the ground-based values, which is close to the combined uncertainty of ground-based NDACC measurements and of the comparison method. Under many conditions, day-to-day fluctuations of the stratospheric NO_2 column seem to be smoothed by GOME-2C, in comparison to the fluctuations reported by ground-based instruments. Variations of the stratospheric NO_2 column at seasonal scale are captured consistently by all measurement systems. Further investigation based on reprocessed ground-based data with state-of-the-art algorithms needs to be done to confirm current provisional conclusions on GOME-2C data quality and to elucidate apparent dependences on SZA in more difficult conditions.

- Preliminary validation results for GOME-2C and GOME-2B tropospheric and total NO_2 columns are generally very similar, even if the regression parameters can be slightly different. GOME-2 data are able to measure total and tropospheric NO_2 columns and its temporal evolution, especially in sub-urban and remote conditions, while larger under-estimation is found with respect to ground-based MAXDOAS and DirectSun measurements performed in urban environment. This is partially inherent to the large GOME-2 pixel size (40 x 80 km²), not representative of the local urban NO_2 pattern sampled by the ground-based instruments, as already showed in past validation exercises (NO2 ACSAF VR 2017; Pinardi et al., in preparation). From the MAXDOAS monthly mean values scatter plot, a global correlation coefficient of 0.83 is obtained for GOME-2C, with a slope of about 0.49, strongly influenced by the large ground-based columns in Mexico. Better results are obtained when only focusing in remote and suburban locations, with correlation of 0.92 and slope of 0.75. Compared to Pandora direct-sun measurements, GOME-2C and GOME-2B results are quite coherent, with correlation coefficients of 0.89 and 0.75 and regression slopes smaller than 0.5.

Further improvement of the operational NO_2 product could be obtained on all GOME-2 instruments by implementing outcomes of scientific investigations (Liu et al., 2019a; 2019b) into the UPAS operational processor, but this is out of the scope of the present document.

F. REFERENCES

F.1. Applicable documents

[ATBD] Algorithm Theoretical Basis Document - GOME-2 Total Column Products of Ozone, NO_2, BrO, HCHO, SO_2, H_2O, OClO, and Cloud Properties (GDP 4.8 for GOME-2A&-B; GDP 4.9 for GOME-2C), Valks, P., Loyola D., Hao N., Hedelt, P., Slijkhuis S., Gross, M., Gimeno Garcia, S., Lus, R., 2019,

[PUM] Valks, P., et al., (2017), Product User Manual for GOME Total Column Products of Ozone, NO2, BrO, HCHO, SO2, H2O, OClO and Cloud Properties, (GDP 4.8 for GOME-2A&-B; GDP 4.9 for GOME-2C) , SAF/AC/DLR/PUM/01, Iss. 3/B, , Nov, 2019,

[SESP] Service Specification Document, SAF/AC/FMI/RQ/SESP/001/issue 1.3, Hovila, J., Hassinen, S., 17 June 2019. https://acsaf.org/docs/AC_SAF_Service_Specification.pdf

[VIM] Joint Committee for Guides in Metrology (JCGM/WG 2) 200:2008 & ISO/IEC Guide 99-12:2007, International Vocabulary of Metrology – Basic and General Concepts and Associated Terms (VIM), http://www.bipm.org/en/publications/guides/vim.html

[GUM] Joint Committee for Guides in Metrology (JCGM/WG 1) 100:2008, Evaluation of measurement data – Guide to the expression of uncertainty in a measurement (GUM), http://www.bipm.org/utils/common/documents/jcgm/JCGM_100_2008_E.pdf

[QA4EO] A Quality Assurance framework for Earth Observation, established by the CEOS. It consists of ten distinct key guidelines linked through an overarching document (the QA4EO Guidelines Framework) and more community-specific QA4EO procedures, all available on http://qa4eo.org/documentation.html A short QA4EO "user" guide has been produced to provide background into QA4EO and how one would start implementing it (http://qa4eo.org/docs/QA4EO_guide.pdf)

F.2 Peer-reviewed articles

Boersma, K. G., Eskes, H. J. and Brinksma, E. J.: Error analysis for tropospheric NO_2 retrieval from space, J. Geophys. Res., 109(D4), doi:10.1029/2003JD003962, 2004.

Boersma, K. G., Eskes, H. J., Dirksen, R. J., van der A, R. J., Veefkind, J. P., Stammes, P., Huijnen, V., Kleipool, Q. L., Sneep, M., Claas, J., Leitão, J., et al.: An improved tropospheric NO2 column retrieval algorithm for the Ozone Monitoring Instrument, Atmos. Meas. Tech., 4(9), 2329-2388, doi:10.5194/amt-4-1905-2011, 2011.

Boersma, K. F., Eskes, H. J., Richter, A., De Smedt, I., Lorente, A., Beirle, S., van Geffen, J. H. G. M., Zara, M., Peters, E., Van Roozendael, M., Wagner, T., Maasakkers, J. D., van der A, R. J., Nightingale, J., De Rudder, A., Irie, H., Pinardi, G., Lambert, J.-C., and Compernolle, S. C.: Improving algorithms and uncertainty estimates for satellite NO2 retrievals: results from the quality assurance for the essential climate variables (QA4ECV) project, Atmos. Meas. Tech., 11, 6651–6678, https://doi.org/10.5194/amt-11-6651-2018, 2018.

Brinksma, E. J., et al. (2008), The 2005 and 2006 DANDELIONS NO2 and aerosol intercomparison campaigns, J. Geophys. Res., 113, D16S46, doi:10.1029/2007JD008808.

Celarier, E. A., E. J. Brinksma, J. F. Gleason, J. P. Veefkind, A. Cede, J. R. Herman, D. Ionov, F. Goutail, J-P. Pommereau, J.-C. Lambert, M. van Roozendael, G. Pinardi, F. Wittrock, A. Schönhardt, A. Richter, O. W. Ibrahim, T. Wagner, B. Bojkov, G. Mount, E. Spinei, C. M. Chen, T. J. Pongetti, S. P. Sander, E. J. Bucsela, M. O. Wenig, D. P. J. Swart, H. Volten, M. Kroon, and P. F. Levelt (2008), Validation of Ozone Monitoring Instrument Nitrogen Dioxide Columns, Journal of Geophysical Research – Atmosphere, Vol. 113, doi:10.1029/2007JD008908.

Clémer K., Van Roozendael, M., Fayt, C., Hendrick, G., Hermans, C., Pinardi, G., Spurr, R., Wang, P., and De Mazière, M., (2010) Multiple wavelength retrieval of tropospheric aerosol optical properties from MAXDOAS measurements in Beijing. Atmos. Meas. Tech., **3**, pp 863–878, doi:10.5194/amt-3-863-2010.

Compernolle,S., Verhoelst, T., Pinardi, G., Granville, J., Hubert, D., Keppens, A., Niemeijer, S., Rino, B., Bais, A., Beirle, S., Boersma, F., Burrows, J.P., De Smedt, I., Eskes, H., Goutail, F., Hendrick, F., Lorente, A., Pazmino, A., Piters, A., Peters, E., Pommereau, J.P., Remmers, J., Richter, A., van Geffen, J., Van Roozendael, M., Wagner, T., and Lambert, J.C.: Validation of Aura-OMI QA4ECV NO2 Climate Data Records with ground-based DOAS networks: role of measurement and comparison uncertainties, submitted to ACPD, 2019.

Drosoglou, T., Bais, A. F., Zyrichidou, I., Kouremeti, N., Poupkou, A., Liora, N., Giannaros, C., Koukouli, M. E., Balis, D., and Melas, D.: Comparisons of ground-based tropospheric NO2 MAX-DOAS measurements to satellite observations with the aid of an air quality model over the Thessaloniki area, Greece, Atmos. Chem. Phys., 17, 5829–5849, https://doi.org/10.5194/acp-17-5829-2017, 2017.

Friedrich, M. M., Rivera, C., Stremme, W., Ojeda, Z., Arellano, J., Bezanilla, A., García-Reynoso, J. A., and Grutter, M.: NO2 vertical profiles and column densities from MAX-DOAS measurements in Mexico City, Atmos. Meas. Tech., 12, 2545–2565, https://doi.org/10.5194/amt-12-2545-2019, 2019.

Hendrick, F., Müller, J.-F., Clémer, K., Wang, P., De Mazière, M., Fayt, C., Gielen, C., Hermans, C., Ma, J. Z., Pinardi, G., Stavrakou, T., Vlemmix, T., and Van Roozendael, M. (2014), Four years of ground-based MAX-DOAS observations of HONO and NO2 in the Beijing area, Atmos. Chem. Phys., 14, 765-781, doi:10.5194/acp-14-765-2014.

Herman, J., A. Cede, E. Spinei, G. Mount, M. Tzortziou, and N. Abuhassan (2009), NO_2 column amounts from ground-based Pandora and MFDOAS spectrometers using the direct-sun DOAS technique: Inter-comparisons and application to OMI validation, J. Geophys. Res., 114 (D13307), 10.1029/2009JD011848.

Herman, J., Abuhassan, N., Kim, J., Kim, J., Dubey, M., Raponi, M., and Tzortziou, M.: Underestimation of column NO2 amounts from the OMI satellite compared to diurnally varying ground-based retrievals from multiple PANDORA spectrometer instruments, Atmos. Meas. Tech., 12, 5593–5612, https://doi.org/10.5194/amt-12-5593-2019, 2019.

Ionov, D. V., et al., (2008) Ground-based validation of EOS-Aura OMI NO2 vertical column data in the midlatitude mountain ranges of Tien Shan (Kyrgyzstan) and Alps (France). J. Geophys. Res., 113, D15S08, doi:10.1029/2007JD008659.

Irie, H., Kanaya, Y., Akimoto, H., Tanimoto, H., Wang, Z., Gleason, J. G., and Bucsela, E. J.: Validation of OMI tropospheric NO_2 column data using MAX-DOAS measurements deep inside the North China Plain in June 2006: Mount Tai Experiment 2006, Atmos. Chem. Phys., 8, 6577-6586, doi:10.5194/acp-8-6577-2008, 2008.

Irie, H., Takashima, H., Kanaya, Y., Boersma, K. F., Gast, L., Wittrock, F., Brunner, D., Zhou, Y., and Van Roozendael, M. (2011), Eight-component retrievals from ground-based MAX-DOAS observations, Atmos. Meas. Tech.., 4, 1027-1044 doi:10.5194/amt-4-1027-2011.

Irie, H., Boersma, K. F., Kanaya, Y., Takashima, H., Pan, X., and Wang, Z. F. (2012), Quantitative bias estimates for tropospheric NO_2 columns retrieved from SCIAMACHY, OMI, and GOME-2 using a common standard for East Asia, Atmos. Meas. Tech., 5, 2403-2411, doi:10.5194/amt-5-2403-2012.

Kanaya, Y., Irie, H., Takashima, H., Iwabuchi, H., Akimoto, H., Sudo, K., Gu, M., Chong, J., Kim, Y. J., Lee, H., Li, A., Si, F., Xu, J., Xie, P.-H., Liu, W.-Q., Dzhola, A., Postylyakov, O., Ivanov, V., Grechko, E., Terpugova, S., and Panchenko, M. (2014), Long-term MAX-DOAS network observations of NO2 in Russia and Asia (MADRAS) during the period 2007–2012: instrumentation, elucidation of climatology, and comparisons with OMI satellite observations and global model simulations, Atmos. Chem. Phys., 14, 7909-7927, doi:10.5194/acp-14-7909-2014.

Liu, S., Valks, P., Pinardi, G., De Smedt, I., Yu, H., Beirle, S., and Richter, A.: An improved total and tropospheric NO2 column retrieval for GOME-2, Atmos. Meas. Tech., 12, 1029-1057, https://doi.org/10.5194/amt-12-1029-2019, 2019a.

Liu, S., Valks, P., Pinardi, G., Xu, J., Argyrouli, A., Lutz, R., Tilstra, L. G., Huijnen, V., Hendrick, F., and Van Roozendael, M.: An improved air mass factor calculation for NO2 measurements from GOME-2, Atmos. Meas. Tech. Discuss., https://doi.org/10.5194/amt-2019-265, in review, 2019b.

Lutz, R., D. Loyola, S. Gimeno Garcia, and F. Romahn, OCRA radiometric cloud fractions for GOME-2A/B, Atmos. Meas. Tech., 9, 2357-2379, 2016.

Ma, J. Z., Beirle, S., Jin, J. L., Shaiganfar, R., Yan, P., and Wagner, T.: Tropospheric NO_2 vertical column densities over Beijing: results of the first three years of ground-based MAX-DOAS measurements (2008–2011) and satellite validation, Atmos. Chem. Phys., 13, 1547-1567, doi:10.5194/acp-13-1547-2013, 2013.

Peters, E., Wittrock, F., Großmann, K., Frieß, U., Richter, A., and Burrows, J. P.: Formaldehyde and nitrogen dioxide over the remote western Pacific Ocean: SCIAMACHY and GOME-2 validation using ship-based MAX-DOAS observations, Atmos. Chem. Phys., 12, 11179-11197, doi:10.5194/acp-12-11179-2012, 2012.

Pinardi, G., M. Van Roozendael, F. Hendrick, N. Theys, J.-C. Lambert, J. Granville, A. Cede, Y. Kanaya, H. Irie, F. Wittrock, A. Richter, E. Peters, A. Blechschmidt, T. Wagner, J. Remmers, U. Friess, T. Vlemmix, A. Piters, M. Tiefengraber, J. Herman, N. Abuhassan, R. Holla, A. Bais, N. Kouremeti J. Hovila, J. Chong, O. Postylyakov, J. Ma, P. Valks, F. Boersma, Validation of tropospheric NO2 columns measurements from GOME-2 and OMI using MAX-DOAS and direct sun network observations, in preparation for AMTD.

Richter, A., Begoin, M., Hilboll, A. and Burrows, J. P.: An improved NO2 retrieval for the GOME-2 satellite instrument, Atmos. Meas. Tech., 4(6), 213-246, doi:10.5194/amt-4-1147-2011, 2011.

Richter, A., M. Weber, J. P. Burrows, J.-C. Lambert, and A. van Gijsel (2013), Validation Strategy for Satellite Observations of Tropospheric Reactive Gases, Annals of Geophysics, Vol. 56, 10.4401/AG-6335.

Tzortziou M., Herman, J.R., Cede, A., Loughner, C.P., Abuhassa, N., Naik, S. (2013), Spatial and temporal variability of ozone and nitrogen dioxide over a major urban estuarine ecosystem, J. Atmos. Chem., DOI 10.1007/s10874-013-9255-8.

Valks, P., Pinardi, G., Richter, A., Lambert, J.-C., Hao, N., Loyola, D., Van Roozendael, M. and Emmadi, S.: Operational total and tropospheric NO2 column retrieval for GOME-2, Atmos. Meas. Tech., 4(7), 1491-1514, doi:10.5194/amt-4-1491-2011, 2011.

Vandaele, A.C., et al.: High-resolution Fourier transform measurement of the NO_2 visible and near-infrared absorption cross-section: Temperature and pressure effects, J. Geophys. Res., 107, D18, 4348, doi:10.1029/2001JD000971, 2002.

Vlemmix, T., Piters, A. J. M., Stammes, P., Wang, P., and Levelt, P. F. (2010), Retrieval of tropospheric NO_2 using the MAX-DOAS method combined with relative intensity measurements for aerosol correction, Atmos. Meas. Tech., 3, 1287-1305, doi:10.5194/amt-3-1287-2010.

Vlemmix, T., Hendrick, F., Pinardi, G., De Smedt, I., Fayt, C., Hermans, C., Piters, A., Levelt, P., and Van Roozendael, M. (2014), MAX-DOAS observations of aerosols, formaldehyde and nitrogen dioxide in the Beijing area: comparison of two profile retrieval approaches, Atmos. Meas. Tech. Discuss., 7, 9673-9731, doi:10.5194/amtd-7-9673-2014.

Wagner, T., Beirle, S., Brauers, T., Deutschmann, T., Frieß, U., Hak, C., Halla, J. D., Heue, K. P., Junkermann, W., Li, X., Platt, U., and Pundt-Gruber, I. (2011), Inversion of tropospheric profiles of aerosol extinction and HCHO and NO2 mixing ratios from MAX-DOAS observations in Milano during the summer of 2003 and comparison with independent data sets, Atmos. Meas. Tech., 4, 2685-2715, doi:10.5194/amt-4-2685-2011.

F.3 Technical notes and presentations

NO_2 ACSAF VR 2017: Pinardi, G., Lambert, J.-C., Yu, H., De Smedt, I., Granville, J., van Roozendael, M. and Valks, P., Validation report of Level-2 (NRT, offline, reprocessed) and Level-3 GOME-2 NO2 column products (GDP 4.8) for MetOp-A and –B, SAF/AC/IASB/VR/NO2, November 2017, https://acsaf.org/docs/vr/Validation_Report_NTO_OTO_DR_L3_NO2_Nov_2017.pdf

Lambert, J-C., et al., (2004) Geophysical Validation of SCIAMACHY NO2 Vertical columns: Overview of Early 2004 Results. Proc. Atmospheric Chemistry Validation of Envisat-2, ESA/ESRIN, 3-7 May 2004, Frascati, Italy.

Lambert, J.-C., (2006) Télédétection spatiale ultraviolette et visible de l'ozone et du dioxyde d'azote dans l'atmosphère globale. PhD Thesis, Faculté des sciences appliquées/Ecole polytechnique, Free University of Brussels, 291 pp.

Pinardi, G., Lambert, J.C., Granville, J., Van Roozendael, M., Delcloo, A., De Backer, H., Valks, P., Hao, N., (2010) OVERVIEW OF THE VALIDATION OF GOME-2 TOTAL AND TROPOSPHERIC NO2 COLUMNS, proceeding of the EUMETSAT Meteorological Satellite Conference, 9-12 September 2010, Cordoba, Spain.

Pinardi, G., Van Roozendael, Lambert, J.C., Clemer, K., De Smedt, I., Hendrick, G., Lerot, C., Theys, N., van Gent, J., Vlemmix, T., De Maziere, M., De Backer, H., Delcloo, A., Yu, H., INTEGRATED TRACE GAS VALIDATION AND QUALITY ASSESSMENT SYSTEM FOR THE EUMETSAT POLAR SYSTEM, proceeding of the EUMETSAT Meteorological Satellite Conference, 3-7 September 2012, Sopot, Poland.

Pinardi, G., Van Roozendael, M., Lambert, J.-C., Granville, J., Hendrick, F., Tack, F., Yu, H., Cede, A., Kanaya, Y., Irie, I., Goutail, F., Pommereau, J.-P., Pazmino, A., Wittrock, F., Richter, A., Wagner, T., Gu, M., Remmers, J., Friess, U., Vlemmix, T., Piters, A., Hao, N., Tiefengraber, M., Herman, J., Abuhassan, N., Bais, A., Kouremeti, N., Hovila, J., Holla, R., Chong, J., Postylyakov, O., Ma, J., GOME-2 TOTAL AND TROPOSPHERIC NO2 VALIDATION BASED ON ZENITH-SKY, DIRECT-SUN AND MULTI-AXIS DOAS NETWORK OBSERVATIONS, proceeding of the EUMETSAT Meteorological Satellite Conference, 22-26 September 2014, Geneva, Switzerland.

Pinardi, G., M. Van Roozendael, F. Hendrick, S. Compernolle, J.-C. Lambert, J. Granville, C. Gielen, A. Cede, Y. Kanaya, H. Irie, F. Wittrock, A. Richter, E. Peters, T. Wagner, J. Remmers, U. Friess, T. Vlemmix, A. Piters, M. Tiefengraber, J. Herman, N. Abuhassan, R. Holla, A. Bais, D. Balis, T. Drosoglou, N.

Kouremeti, J. Hovila, J. Chong, O. Postylyakov, A. Borovski, J. Ma, Satellite nadir NO2 validation based on direct-sun and MAXDOAS network observations, oral presentation at the DOAS workshop, September 2017, Yokohama, Japan.

Operation Reports (Op.Rep. 2019a): OPERATIONS REPORT, Issue 1/2019, Reporting period: January – June 2019, https://acsaf.org/docs/or/AC_SAF_Operations_Report_1-2019.pdf, Sept 2019.

Richter, A.,T. Bösch, S. Noel, M. Weber, H. Bovensmann, J. Burrows, Evaluation of GOME2C L1 quality using non-operational L2 retrievals, Presentation at GSAG #53, EUMETSAT, 20 May 2019.